T.R.
GEBZE TECHNICAL UNIVERSITY
INSTITUTE OF BIOTECHNOLOGY

IDENTIFICATION OF THERAPEUTIC TARGETS OF ORLISTAT RELATED TO LKB1/AMPK/ULK1/MTOR SIGNAL AXIS IN PROSTATE CANCER CELLS

AYYÜCE SEVER
A THESIS SUBMITTED FOR THE DEGREE OF
MASTER OF SCIENCE
INSTITUTE OF BIOTECHNOLOGY

GEBZE
2022

T.R.

GEBZE TECHNICAL UNIVERSITY

INSTITUTE OF BIOTECHNOLOGY

IDENTIFICATION OF THERAPEUTIC TARGETS OF ORLISTAT RELATED TO LKB1/AMPK/ULK1/MTOR SIGNAL AXIS IN PROSTATE CANCER CELLS

AYYÜCE SEVER

A THESIS SUBMITTED FOR THE DEGREE OF MASTER OF SCIENCE

INSTITUTE OF BIOTECHNOLOGY

THESIS SUPERVISOR

PROF. DR. ELİF DAMLA ARISAN

GEBZE

2022

T.C.
GEBZE TEKNİK ÜNİVERSİTESİ
BİYOTEKNOLOJİ ENSTİTÜSÜ

PROSTAT KANSERİ HÜCRELERİNDE LKB1/AMPK/ULK1/MTOR SİNYAL EKSENİ İLE İLGİLİ ORLİSTAT TERAPÖTİK HEDEFLERİNİN BELİRLENMESİ

AYYÜCE SEVER
YÜKSEK LİSANS TEZİ
BİYOTEKNOLOJİ ENSTİTÜSÜ

DANIŞMANI
PROF. DR. ELİF DAMLA ARISAN

GEBZE

2022

GEBZE TEKNİK ÜNİVERSİTESİ	YÜKSEK LİSANS JÜRİ ONAY FORMU

GTÜ Biyoteknoloji Enstitüsü Yönetim Kurulu'nun tarih ve sayılı kararıyla oluşturulan jüri tarafından 20/07/2022 tarihinde tez savunma sınavı yapılan Ayyüce Sever' in tez çalışması Biyoteknoloji Anabilim Dalında YÜKSEK LİSANS tezi olarak kabul edilmiştir.

JÜRİ

ÜYE (TEZ DANIŞMANI)	: Prof. Dr. Elif Damla ARISAN
ÜYE	: Doç.Dr. Pınar OBAKAN YERLİKAYA
ÜYE	: Dr. Öğr. Üyesi Ümit Barış KUTMAN

ONAY

Gebze Teknik Üniversitesi Biyoteknoloji Enstitüsü Yönetim Kurulu'nun …/…/….. tarih ve …../… sayılı kararı.

SUMMARY

Obesity is one of the major risk factors in the development, aggressivity, and metastatic profile of prostate cancer. It was shown that obesity increases the aggressivity of cancer by generating a drug resistance. Therefore, approaches for obesity treatment may be a promising to understand the regulatory role of lipogenesis and adipogenesis pathways. Orlistat activates AMPK by inhibiting Fatty Acid Synthase enzyme, induces apoptosis showing anti-proliferative effects in cancer development by creating toxic effects in cancer cells.

AMPK is a cellular energy sensor that affects cell fate. AMPK activation regulates cellular metabolism by acting on metabolic checkpoints. The hypothesis of our research project is that as it is known to regulate the LKB1-AMPK signalling pathway, cell proliferation, metabolism, and survival events in response to nutrient and energy levels, orlistat will change the behaviour of the associated molecules in the AMPK-LKB1 signalling cascade due to FASN inhibition and have therapeutic potential. For this purpose, we generated stable AMPK$^{-/-}$ PC3 and LNCaP prostate cancer cell lines using CRISPR/Cas9 system to compare orlistat-based alterations in a comparison with wt PC3 and LNCaP cells.

We demonstrated that, AMPK deficiency down-regulates lipid secretion in prostate cancer cells. Besides, higher dose of orlistat was required for the death of AMPK $^{-/-}$ cells compared to the wt cells and selected dose of orlistat reduces colony formation potential in both wt and AMPK$^{-/-}$ prostate cancer cell lines. Additionally, we observed the reduction in mitochondrial activity and induction cell death by damaging cellular membranes as a result of treatment.

Key Words: Prostate cancer, Orlistat, AMPK, Apoptosis, Autophagy, Cancer Metabolism

ÖZET

Obezite, prostat kanserinin gelişimi, agresifliği ve metastatik profilindeki başlıca risk faktörlerinden biridir. Son çalışmalar, obezitenin kanserin agresif olgusunu artırarak bir ilaç direnç mekanizması geliştirdiğini göstermiştir. Bu nedenle, obezite tedavisine yönelik ilaçlar, lipogenez ve adipogenez yollarında farklı hedeflerin düzenleyici rolü nedeniyle umut verici bir konu olabilir. Orlistat, FASN inhibitörü olduğu için AMPK'yı aktive eder. Normal hücrelere zarar vermeden kanser hücrelerinde toksik bir etki yaratır ve kanser gelişiminde anti-proliferatif etki göstererek apoptoz indüklenmesine sebep olur.

AMPK, hücre hayatta kalma ve ölüm kararını etkileyen bir hücresel enerji sensörüdür. AMPK aktivasyonu, metabolik kontrol noktalarına etki ederek hücresel metabolizmayı düzenler. Araştırma projemizin hipotezi, LKB1-AMPK sinyal yolu, hücre silahlanma, metabolizmayı düzenlemek ve besin ve enerji seviyelerine tepki olarak hayatta kalma olayları olan orlistat, FASN engellemesi nedeniyle AMPK-LKB1 sinyal kaskadlarındaki ilgili moleküllerin davranışını değiştirecek ve terapötik potansiyele sahip olacaktır. Bu amaçla, PC3 ve LNCaP hücrelerine kıyasla Orlistat tabanlı değişiklikleri karşılaştırmak için CRISPR/Cas9 sistemini kullanarak stabil $AMPK^{-/-}$ PC3 ve LNCaP prostat kanseri hücre hatları oluşturduk.

AMPK eksikliğinin prostat kanser hücrelerindeki lipit salgısı düzenlemesini gösterdik. Ayrıca, doğal tip hücrelere kıyasla $AMPK^{-/-}$ hücrelerinin ölümü için daha yüksek Orlistat dozunun gerekli olduğu da belirlendi. Bunun yanında, seçilen Orlistat dozu hem dt hem de $AMPK^{-/-}$ prostat kanser hücresi hatlarında koloni oluşma potansiyelini azalttığını tespit ettik.

Anahtar Kelimeler: Prostat Kanseri, Orlistat, AMPK, Apoptoz, Otofaji, Cancer Metabolism

ACKNOWLEDGEMENTS

I wish to show my appreciation to dear Prof. Dr. Elif Damla ARISAN for giving me an opportunity to be a candidate for MSc., leading and teaching me during this thesis and being understanding and supportive even when I don't believe in myself.

I wish to extend my special thanks to Dr. Hüseyin BALCI, for all his contributions to my studies during laboratory. I would like to thank Mustafa Doğukan METİNER for his valuable support, for sharing his experience in wet lab work patience, and kindly behavior. He shared plenty of valuable experiences and ideas. I would like to thank my beloved friends Burçin ÖZBEKLE and Gizem KUGU for their endless support.

I would like to thank my lovely parents, Emel SEVER and Zeki SEVER, and my dear sister Aybike SEVER for their faith in me, love, and support.

This study was funded by The Scientific and Technological Research Council of Turkey (TUBITAK) with the Project Number of 221Z099.We would like to thank TUBITAK for providing funds within the scope of this project.

TABLE of CONTENTS

LIST of ABBREVIATIONS and ACRONYMS

Abbreviations and Acronyms		Explanations
α	:	Alpha
β	:	Beta
µ	:	micro
µg	:	microgram
µl	:	microlitre
µM	:	micromolar
µm	:	micrometre
ACC	:	Acetyl coenzym carboxylase
ACLY	:	ATP citrate lyase
ADT	:	Androgen Deprivation Therapy
AICAR	:	5-Aminoimidazole-4-carboxamide ribonucleotide
AMPK	:	AMP-activated protein kinase
Apaf-1	:	Apoptotic protease activating factor
APS	:	Ammonium persulfate
AR	:	Androgen Receptor
BSA	:	Bovine serum albumin
CaMKKB	:	Calcium/calmodulin dependent protein kinase
CRISPR	:	Clustered Regularly Interspaced Short Palindromic Repeats
DNA	:	Deoxyribonucleic acid
FAS	:	Fatty acid synthase enzyme
FBS	:	Fetal Bovine Serum
LKB1	:	Liver Kinase Beta 1
LNCaP	:	Lymph Node Carcinoma of the Prostate
MAPK	:	Mitogen activated protein kinase
mTORC1	:	mTOR complex 1
MTT	:	3-(4,5-dimetiltriazol-2-il)-2,5-difeniltetrazolium bromid
MW	:	Molecular Weight
PARP	:	ADP-ribose polimerase
PBS	:	Phosphate buffer saline
PC3	:	Prostate cancer

PI3K	:	Phosphoinositide 3- kinase
PSA	:	Prostate specific antigen
PVDF	:	Polyvinylidene fluoride
Raptor	:	mTOR-related regulatory protein
SREBP	:	Sterol regulatory element- binding proteins
TNF	:	Tumor necrosis factor
TNFR1	:	TNF receptor-1

LIST of FIGURES

LIST of TABLES

1. INTRODUCTION

1.1. What is Prostate Cancer?

Prostate cancer (PCa) is an important health problem that involves approximately 1,6 million new cases diagnosed with and 366,000 men die of prostate cancer worldwide every year [1]. There are 10 million men suffering from prostate cancer and 700,000 of them are in metastatic level [2]. The risk factors that are seen as robust markers of prostate cancer are not certain. Prostate cancer ranks the third leading cause of death among men in America after lung and colorectal cancer. According to the American Cancer Society, for the data of 2017, it is estimated that, about 161,360 new cases of prostate cancer will strike and about 26,730 deaths will come because of the disease [3]. The location of prostate tumor in prostate gland to generation of prostate cancer was shown in Figure 1.1.

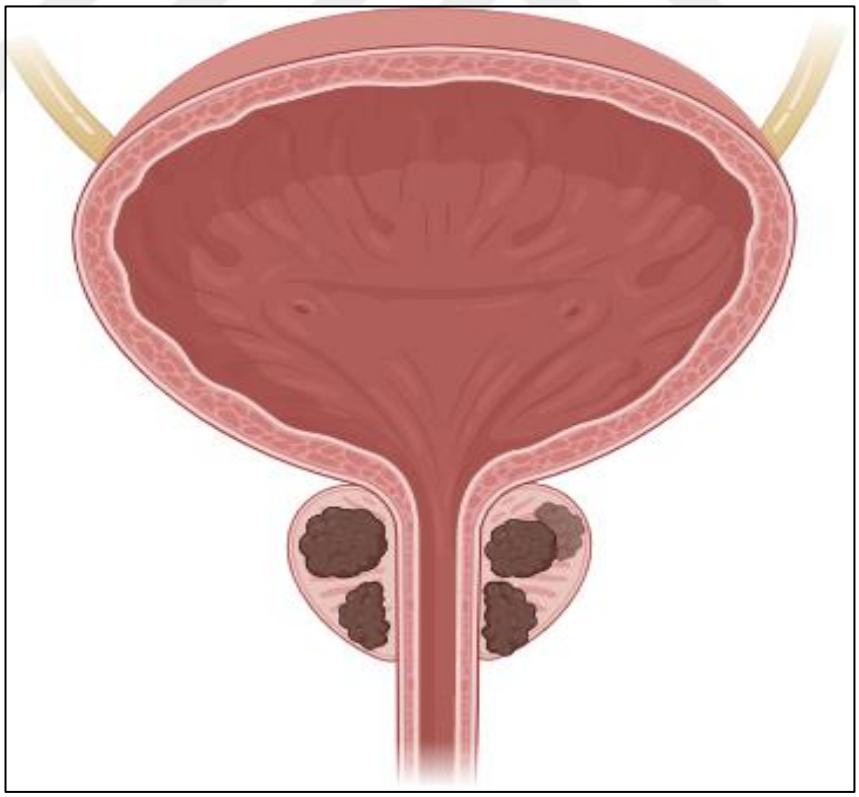

Figure 1. 1: Figure shows the location of prostate tumor for generation of prostate cancer.

Basically, abnormally dividing cells in prostate gland is the marker of prostate cancer resulting in abnormal prostate gland growth. The abnormal proliferation and growth of cancer cells that generate the prostate cancer was shown in Figure 1.2. Although natural initiation of the disease is unclear, disease progression is determined by the stage and the level of tumor [4]. It will affect the life standard of men because of slow growing tumor, but most men don't die from the prostate cancer. Improved treatment strategies would alleviate the symptoms of the disease. Mostly, metastasis is the source of deaths because when the cancerous cells spread to the other body parts including pelvic and retroperitoneal lymph nodes, the spinal cord, bladder, rectum, bone, and brain [3]. Figure 1.2 shows the neoplastic growth stages of a tumor.

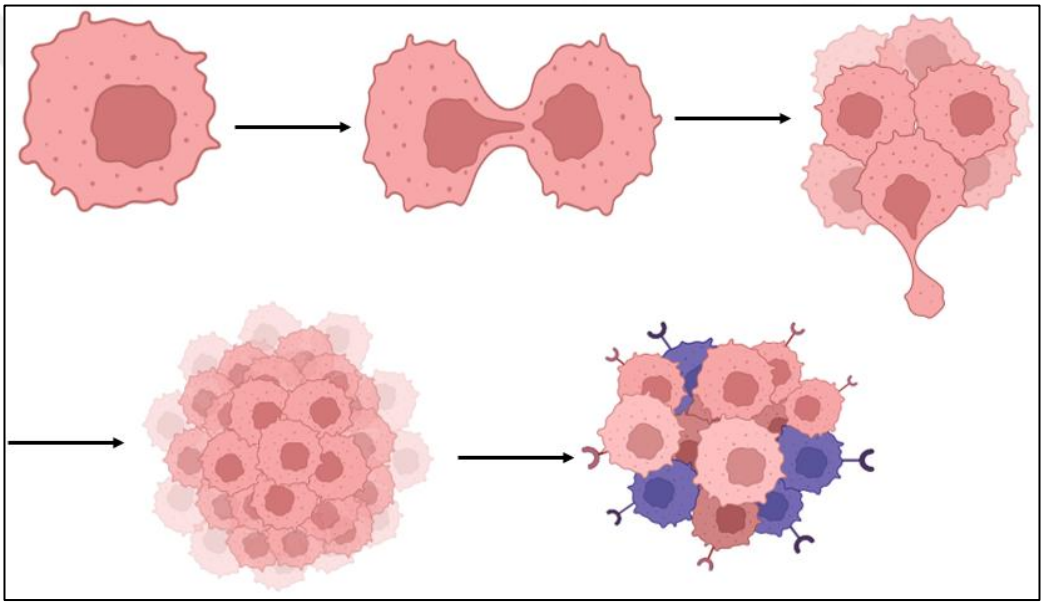

Figure 1. 2: The accumulation of somatic mutations in certain genes are the cause of tumor cells, which associated with neoplastic growth.

Oncogenic potential of prostate cancer is associated with basically three complex interactions such as inherent germline susceptibility, acquired somatic gene alterations and environmental factors [2]. When it comes to the biological approach, the adult human prostate has three main parts, which are central, transition and peripheral zones. Mostly, prostate tumors arise at the outermost peripheral zone [2].

High-grade lesions are stated to be initiators by resembling adenocarcinomas after genetically modified. DNA damage of mutated cells with chronic inflammation and infection accompanies by reactive oxygen species are the driving forces for developing prostate cancer [2].

Finally, proliferative epithelial cells lead to neoplastic growth and malignancy through genomic and epigenetic changings [2]**.**

Although there are no certain ways, other than some dietary options including nutrition and lifestyle changing, to end the prostate cancer, it is expected that men with prostate cancer will increase in the future. Therefore, it is important to find new therapeutic advances like combinatorial therapies to increase the life expectancy. There are some nutrients that are said to decrease the incidence of prostate cancer such as extracts from pomegranate, green tea, broccoli, turmeric, crocetin, curcumin, flaxseed, and soy among others. Besides, sustainable vegan nutrients and exercise are suggested to lower the risks of developing prostate cancer. Unfortunately, these are not very conclusive approaches and dietary applications can have different effects for individuals [3].

Early detection increases the possibility of treatment and allows to discover new clinical trials to manage, control and finally combat the disease in different development stages [5].

1.1.1. Epidemiology of Prostate Cancer

Globally, prostate cancer is the fifth most common reason of cancer death, and the burden ranks among the top five cancers for incidence and mortality. When the patterns of incidence and mortality was analyzed, the role of individual risk factors and the behaviors of population can be illustrated to understand the burden of the disease [1].

Risk factors in prostate cancer development can be studied in broad spectrum. Although there aren’t any certain agents that cause prostate cancer, small number of risks factors have been characterized but they have both contradictory or inconclusive results accompanied by small studies [4].

1.1.2. Prevalence

Prostate cancer is relatively common in developed countries. According to the Global Burden of Disease Cancer Collaboration, with low- middle sociodemographic countries, the probability of prostate cancer diagnosis by age 79, are one in 47 among countries compared with one in six among countries with high sociodemographic index [1] , [4]. According to the Cancer Research UK, the incidence of prostate cancer cases increases dependent on the age. Between 75-79 means highest interval with 751 per 100,000 for ages 55-59, the incidence was 155 per 100,000 [4].

Besides, global variations have significant role in cancer incidence. While the highest rate is seen in African- American men in the United States, Asian men who live in their native countries have the lowest rate. There is a 40- fold difference in age-related prevalence between the highest and the lowest [1], [6]. The dependence of age can be associated with prostate specific antigen (PSA) screening, which is highly related with lifestyle factors in disease risk. For instance, prostate cancer prevalence increases when migration to the high- risk countries from low- risk countries is augmented [6]. The map of age associated prostate cancer prevalence was shown in Figure 1.3.

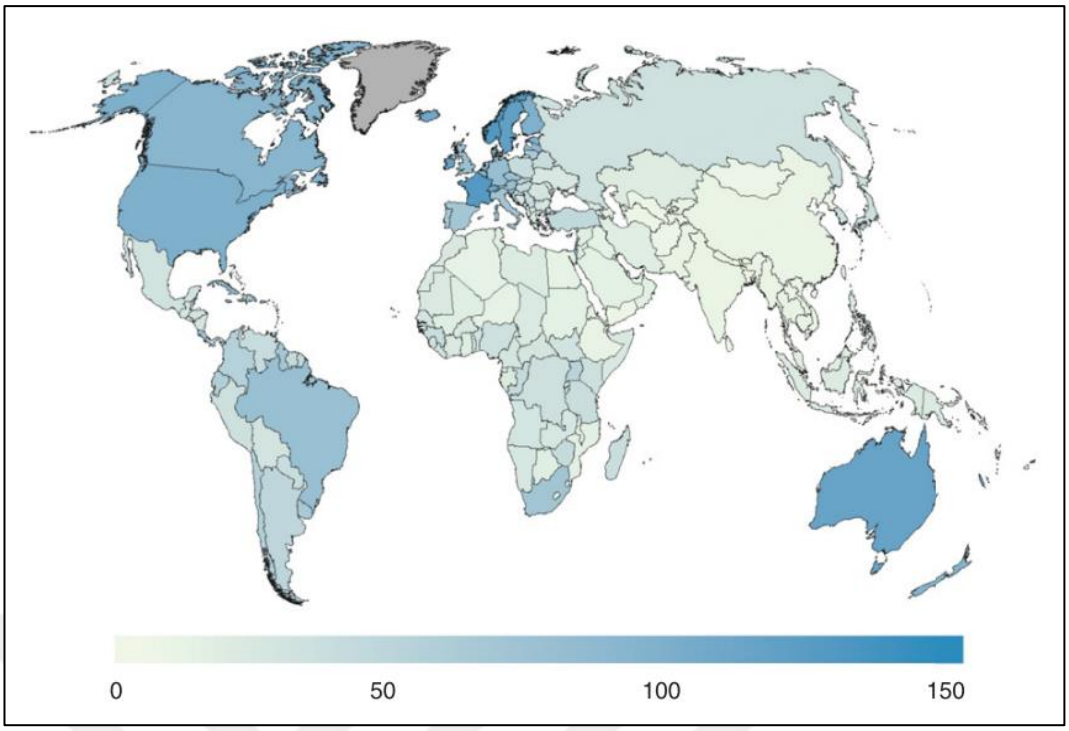

Figure 1. 3: The map of age- associated prostate cancer prevalence worldwide. Rates of prevalence were presented per 100.000 in the population and age- adjusted in order to make comparison between countries.

Introduction of PSA screening has a role observing high incidence rate. Therefore, it can be said that the more PSA screening becomes popular worldwide, the more prostate cancer case is observed [1].

1.1.3. Mortality

Prostate cancer is one of the most common cancers with fifth most common cause of cancer related death, globally. According to the global mortality patterns, it is clear that less developed regions, such as Caribbean, Middle and Southern Africa, experience higher mortality rates than developed regions, such as Asia, especially Eastern and South-Central Asia, caused by prostate cancer [1].

There have been significant reductions in the mortality rates of prostate cancer, but the reason is unclear. PSA screening can be the most important reason because of the potential of earlier detection and finally earlier treatment modalities. Recent changes are the mortality rates are the result of both incidence and the survival rates among patients [1].

1.1.4. Risk Factors for Prostate Cancer

There were few certain risk factors for developing prostate cancer, such as age, race, and genetic susceptibility. Basically, prostate cancer occurs because of complex interaction of age, endogenous hormone balance, genetic factors and environmental factors such as nutrition [4]. According to Genome wide association studies (GWAS), there are more than 180 genetic risk loci, that increase the likelihood of developing prostate cancer. Surprisingly, being tall was stated as a risk factor [1]. Risk factors provide information about the possible mechanisms related with prostate cancer [1].

Age is said to be one of the most important risk factors that is associated with prostate cancer. It was stated that, the disease is quite rare among men younger than 40 years of age. After 55 years of age, the rate dramatically increases, not only low but also highly developed regions [1].

Ethnicity and race are significant factors of developing prostate cancer. For instance, there is a threefold difference in incidence rates of prostate cancer across race/ethnicity groups in the United States, with the highest prevalence among black men, parallel with the mortality rates [1].

Genetic susceptibility for PCa is strong evidence of developing prostate cancer. Men with a positive family history have two- to threefold higher risk than men with negative family history [1]. Surprisingly, family history of breast cancer is even associated with developing prostate cancer. According to the epidemiological studies, there are two prostate cancers, which are hereditary prostate cancer with autosomal dominant trait and familial prostate cancer without mendelian trait. Hereditary prostate cancer based on altered gene that cause the increment of disease susceptibility and is associated with familial history by the accumulation of mutant gene. Therefore, it can be said that genetic susceptibility is considered as a risk factor [4].

Obesity is one of the major public health issues. According to World Health Organization, the prevalence of obesity worldwide has more than doubled since 1980. There were 1.9 billion overweight adults and 600 million of them was considered as obese. Obesity has a great impact on people’s life, which arises from abnormal regulation of hormonal pathways, leads upregulation of insulin, estradiol, inflammatory cytokines and downregulation of adiponectin, testosterone and sex hormone binding globulin.

The body size and the incidence are associated with the mortality of cancer. Besides, biomarkers have been characterizing this relationship vividly to visualize the mechanisms that affect prostate cancer initiation and progression [1]. Obesity was stated as a risk factor, which was shown as a representative as Figure 1.4.

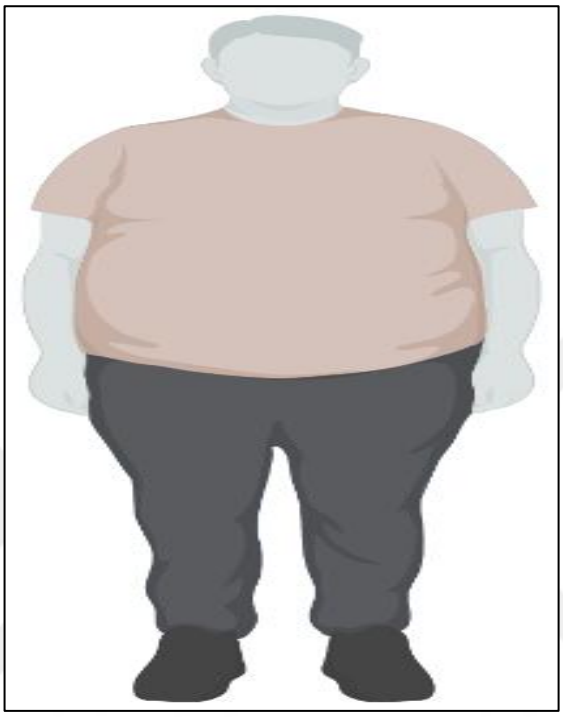

Figure 1. 4: Obesity or being overweight increases the risk of developing prostate cancer.

According to prospective cohort studies, regular exercise decreases the risk of developing fatal prostate cancer. They stated that men with dynamic activities had 77% lower risk of advanced prostate cancer. They also found that men who exercised dynamically for at least 3 hours had 61% lower risk of prostate cancer related death, when compared with men with 1 hour per week of dynamic activity. Although, these studies were performed based on the vigorous activity, both vigorous and non-vigorous activity has a role for reducing the prostate cancer related mortality risk. Although, molecular mechanism underlying this relation is not clear, there may be alterations in sex hormone levels and anti-inflammatory pathways [1].

Smoking is one of the major health problems that has also impact on prostate cancer. According to U.S. Surgeon General, there is “suggestive” evidence that states smoking increase not only cancer progression but also the risk of prostate cancer death.

Current smokers had 60% higher risk of prostate cancer related mortality when compared with men who never smoked. Surprisingly, when current treatment modalities such as radiation, androgen deprivation therapy (ADT) and radical prostatectomy are applied, the prostate cancer progression becomes worse on men with smoking history [1]. Smoking was stated as a major risk factor, which was shown as a representative as Figure 1.5.

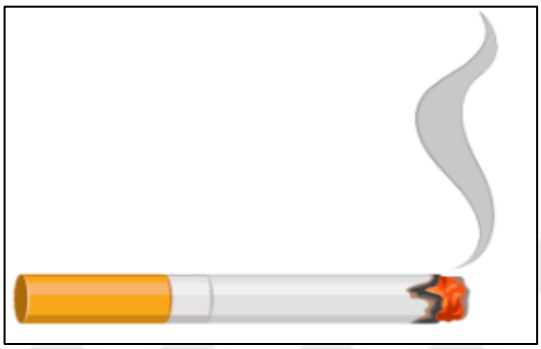

Figure 1. 5: Smoking is one of the causes of prostate cancer it may weaken the body's immune system, which causes ungoverned growth of cancers.

Nutrition is one of the major components that affects prostate cancer. Although it is not clear, there are several associations between diet and prostate cancer progression especially fat and grain intake [4]. The quality of nutrition is one of the important risk factors for developing prostate cancer, which was shown as a representative image as Figure 1.6.

Figure 1. 6: Fat and grain intake is associated with prostate cancer progression.

Dietary options are quite effective to cope with prostate cancer. They either alleviate the symptoms or reduce the risk of developing the disease by targeting certain

molecular pathways. Oxidative stress is associated with carcinogenesis through protein and DNA damage [1].

Lycopene is considered as a strong antioxidant and has a potential to accumulate in a prostate tissue in order to restrict the damaging effects of oxidative stress and eventually reduce the carcinogen effects. Not only lycopene but also lycopene rich foods such as pink grapefruit, watermelon and tomato may have protective roles on prostate cancer. Besides, it was stated that high amount of lycopene lowers angiogenic potential of tumors [1], [4].

Although it was believed, the higher amount of lycopene uptake, the lower the risk of developing prostate cancer, further investigation is needed for indolent disease. Coffee is another antioxidant that has various bioactive compounds that may be associated with the prostate cancer progression. It is believed that coffee has an impact on prostate cancer epidemiology. Surprisingly, some studies showed null results, which means there may be no association between the disease progression and coffee consume. Therefore, there is no certain evidence that states the association between coffee and prostate cancer progression and aggressivity [1].

Additionally, there is a certain mineral believed to make the prostate cancer more aggressive, which is calcium. Although according to the National Health and Nutrition Examination Survey (NHANES) higher calcium intake means higher risk of fatal prostate cancer, some of them could not find any association between the amount of calcium and the aggressivity of prostate cancer [1].

Besides, dairy products, which are the major source of calcium, has been stated as a risk factor. Therefore, it can be said that there is a strong relationship between higher milk or dairy product consume and aggressivity of prostate cancer[1]. Recently, hormones are believed to be associated with prostate cancer but there isn’t any clear evidence that support this involvement. In spite of this improvability, there are certain biomarkers that supports this relation. During prostate cancer, testosterone and dihydrotestosterone levels are increased when compared with the healthy tissue. In prostate cancer cells, steroid hormone receptors are upregulated. Besides, oestrogen therapy has positive effects on prostate cancer treatment. Although the evidence are not clear, excessive amounts of dairy products are stated to be risk factor [4].

1.2. PSA Screening as a Detection Strategy

Although there is no certain way to treat prostate cancer, it is stated that early detection may alleviate the symptoms and reduce the mortality rate. PSA (prostate specific antigen) is a serine protease, whose production is exclusive for prostatic epithelial cells. The fundamental function of PSA is seminal cloth liquefaction. PSA screening is one of the useful methods, which is a blood test that measures the level of PSA in blood, to observe the presence of the disease. It is a biomarker that detects prostate cancer selectively in order to observe clinical progression of the disease. Prostate specific membrane antigen (PSMA) is a type II transmembrane protein, exerts glutamate-carboxypeptidase activity. Because PSMA is upregulated in prostate cancer, scientists look for the PSMA targeting molecules to inhibit its activity [7]. Although low levels of PSA are produced in non-prostatic tissue, high levels are considered as the biomarker of a neoplastic growth in prostate cancer [8]. Thus, targeting PSA can be a promising treatment modality of prostate cancer in order to develop targeted radiopharmaceuticals [7].

In spite of the fact that, PSA screening is the most useful biomarkers of prostate cancer, it has limitations. Cancer progression is based on the behavior of the tumor, and it relies on the biology of the neoplastic growth [7]. Genomic data reveal the distinct changes, that detect the behavior of the tumor whether it will metastasize or become benign. Because of this dynamic alterations PSA won't be stable. PSA levels in blood can be affected by bunch of factors such as certain medical procedures, prostate infection, and medications. The specificity of the PSA test is not clear because PSA derivatives can be calculated when the PSA levels elevated there might be unnecessary biopsies take place. PSA screening is not only useful for determining the presence or absence of the disease but also visualizing the stage of the prostate cancer [8].

1.2.1 Agents for Treatment of Prostate Cancer

Androgen receptor (AR) is one of the most important driver molecules for the development of prostate cancer. It belongs to the nuclear receptor family and is considered as ligand-dependent transcription factor.

Major androgens dihydrotestosterone (DHT), testosterone or other androgenic steroids are possible ligands of this interaction. Unbound AR located in cell cytoplasm. Once it binds with its ligand, it will pass into the nucleus and generate homodimer after the interaction of DNA -binding domain (DBD) and ligand binding domain (LBD). Once it is dimerized, it recognizes DNA response elements and androgen target genes. Then, a wave of downstream pathways is stimulated by recruiting bunch of proteins and epigenetic factors. Basically, AR receptors recruit molecules only if it is bound by androgens. Therefore, androgen deprivation therapy (ADT) may be an effective treatment modality via blocking AR function with competitive antagonists or reducing androgen synthesis in order to impede the spread of prostate cancer. Unfortunately, ADT is a transient option because tumors develop drug resistance. Currently, scientists are investigating new AR antagonists to treat single or combination with other drugs [9].

Docetaxel was one of the most popular agents that is used to treat prostate cancer, which is a chemotherapeutic inhibitor of microtubule de-polymerization. Although it offers prolongation in survival rates, when it was used to cure prostate cancer, acquired drug resistance has emerged. There are five novel agents that were developed recently to help treatment of prostate cancer, such as Sipuleucel-T, Cabazitaxel, Abiraterone Acetate and Enzalutamide [10].

Sipuleucel-T is a cellular immunotherapy that consists of autologous peripheral blood mononuclear cells (PBMC) with leukapheresis. It is based on the reinjection of patient's own PBMC after culturing with a recombinant human protein (PZP-GM-CSF), consisting of prostatic acid phosphatase linked to granulocyte- macrophage colony-stimulating factor [10].

Cabazitaxel, is a novel tubulin- binding taxane, that is efficient for docetaxel-resistant tumors [10].

Abiraterone Acetate was offered to prostate cancer patients who have already treated with docetaxel. Abiraterone is an inhibitor, based on an enzyme with 2 different activities [10].

There should be an enzymatic activity that based on the conversion of pregnenolone and progesterone to 17-OH pregnenolone and 17-OH progesterone and eventually testosterone. Besides, it is used to suppress and stop androgen production at several body parts even in prostate tumors [9], [10].

Enzalutamide is a second- generation competitive AR antagonist and blocking agent that targets androgen receptor signalling pathway in order to impede the binding of androgens to the receptor via inhibiting the translocation of activated AR by weakening the affinity of activated AR to DNA [10]. Apalutamide is another antagonist that is structurally similar to enzalutamide. It has significant side effects such as rash, fatigue, weight loss etc [9].

Darolutamide has a novel chemical structure that has high affinity to the AR LBD and unique antagonistic activity against AR mutants that is also effective on treatment resistant prostate cancer patients [9].

1.3. Molecular Mechanisms in the Formation and Treatment of Prostate Cancer

Tumor formation and development are triggered by bunch of oncogenic activation, which stimulates neoplastic growth on prostate gland. There is a crosstalk between these molecules meaning that they communicate and trigger other signalling molecules causing accumulation of mutations to resist therapeutic agents [11]. These molecules are ideal for scientists to discover new therapeutic targets to suppress the progression of prostate cancer and increase the survival rate of patients [12].

1.3.1 Programmed Cell Death

Programmed cell death or apoptosis is a suicidal way that involves the death of cell by itself, that maintains proliferation/homeostasis, differentiation, development, and elimination of harmful cells. It is the most important strategy of cell death, that provides understanding of pathogenesis of diseases and gain new approaches to develop novel drugs because of dysfunctional apoptosis [13].

There are mainly 2 class of pathways in mammals that involves the apoptosis, such as extrinsic, which is death mediated receptor pathway and intrinsic, which is mitochondrial mediated pathway [13].

Extrinsic pathway involves a signal that comes from outside, such as cytotoxic-T cell, that has Fas ligand (FasL). When FasL binds Fas receptor of target cell via, death domains, it sends first apoptotic signal and FADD adaptor molecule (Fas associated death domain) with DED (death effector domain), is recruited and comes to the death domain of ligand. Procaspase 8 became activated to caspase 8. Then they generate a complex, which is called death inducing signalling complex (DISC). Caspase 8 cleaves and activates procaspase 3 to caspase 3, which acts on apoptotic substrates to form active apoptotic effectors, eventually cell death occurs [13].

Intrinsic pathway has 3 distinct stages, which is initiated by bunch of intrinsic stimuli that makes mitochondrial membrane much more permeable to release apoptotic substance, which are activator caspases, in the form of cytochrome C, Smac/DIABLO. Once stress stimuli are recognized by intracellular proteins, BH3-only proteins, which are BAX and BAK, are activated. They trigger the release of cytochrome c, which should connect with apoptosis protease-activating factor 1 (Apaf-1) and form apoptosome complex, which then activates initiator caspases, such as caspase 9. After that, executioner caspase -3 is recruited. Finally, cell demolition occurs [13].

1.3.2. PI3K-AKT-mTOR Signalling Pathway

Most of the prostate cancer cases, PI3K-AKT-mTOR signalling pathway is found as upregulated. PI3K-AKT-mTOR pathway is a family of proteins whose inhibitors are said to be promising approaches against prostate cancer [7], [11].

PI3Ks are a large family of lipid kinase enzymes that is divided into three main classes, which are Class I, consists of Class IA and Class IB, Class II and Class III based on the substrate specificity and subunit organization. Class IA is responsible for protein localization, receptor binding and activation with its catalytic subunits [11].

When Class IA PI3K is activated, a wave of downstream signalling pathway is triggered via synthesizing the lipid secondary messenger phosphatidylinositol 3,4,5 trisphosphate PIP3 from phosphatidylinositol 4,5 bisphosphate (PIP2) in order to manage cell growth, proliferation autophagy and apoptosis. When the elevated levels of activation, autophagy is downregulated, and neoplastic growth occurs.

Phosphatase and tensin homolog deleted on chromosome 10 (PTEN) as a tumor suppressor, negatively regulates PI3K-AKT-mTOR signalling pathway via converting PIP3 back to PIP2. When PIP3 levels are increased, bunch of kinases such as PDK1 is activated, which cause Akt phosphorylation at residue Thr308. Once Akt is phosphorylated, it starts to regulate vital cellular processes that are maintained by FOXO, GSK3β, Nf-Kβ and TSC2, which directs the inactivation of RHEB, that triggers mTORC1 signalling pathway cause stimulation of cell growth and survival and inhibition of autophagy. Once mTORC1 activated, mTORC2 signalling is regulated indirectly by substrates of mTORC1 in order to mediate cell survival and cell cycle progression. Class II PI3Ks maintain cell migration, channel regulation, endocytosis and exocytosis. The mutation rate of this class of molecules is relatively low. Class II molecules composed of catalytic and regulatory subunits, they regulate autophagy, intracellular and membrane trafficking and AMPK- dependent insulin sensitivity. There is high potential of mutations of molecules for reoccurrence and formation of prostate cancer. Loss of function or loss or inactivation or deregulation of PTEN molecule as a tumor suppressor may take place. AKT molecule may experience alterations such as gain of function, gene amplification via mutations. Also, deregulation of mTORC1 and mTORC2 might cause genetic alterations that results in neoplastic growth. Therefore, it can be stated that, PI3K-AKT-mTOR signalling cascade communicates with multiple cooperative signal transduction pathways to trigger cell survival and tumor growth [7], [11].

According to genomic and transcriptomic profiling studies, genetic mutations in PI3K pathway elements are the causes of prostate cancer that's why it is started to be investigated. Thus, understanding this complex network of molecules help us discover new biomarkers and molecular targets to control, monitor and defeat prostate cancer [7], [11]. Representative image of PI3K-AKT-mTOR signalling pathway was shown in Figure 1.7.

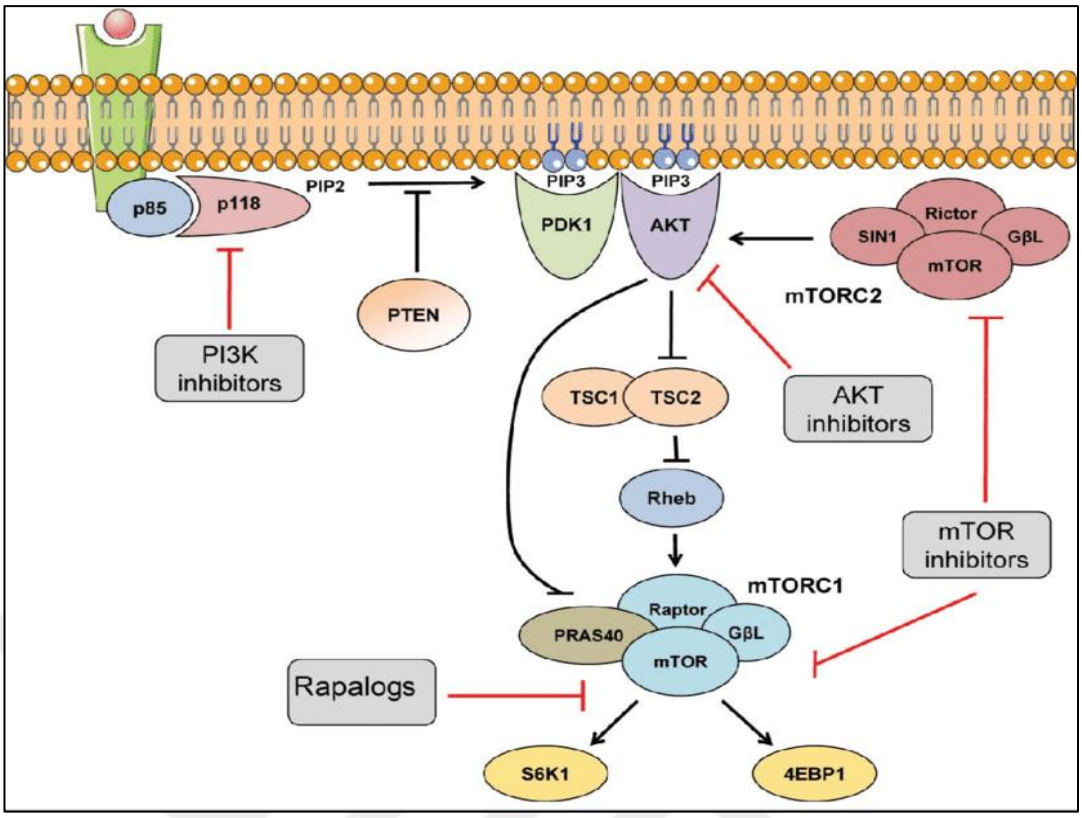

Figure 1. 7: PI3K- Akt-mTOR signalling pathway of family has role for developing prostate cancer, which was found hyperactivated during prostate cancer mostly.

1.4. AMPK

Availability of nutrients and ability to generate ATP by catalytic processes are the main components for cells for maintaining energy balance, unless cellular stress occurs [14], [15]. ATP balance has a major role for mediating homeostasis for being the rechargeable batteries of cells. The AMP activated protein kinase (AMPK) is an energy balance molecule, both cellular and body, that is conserved in essentially all eukaryotes, that means AMPK signalling has a great importance in evolutionary perspective except for few parasites, which detect the amount of available energy in the cell via binding adenine nucleotides directly [16], [17]. AMPK is universally a heterotrimeric molecule, which composed of catalytic α subunit and two regulatory subunits, β and γ [17], [18] α subunit isoforms, which are α1 and α2, are expressed by PRKAA1 and PRKAA2, β subunit isoforms, which are β1 and β2, are expressed by PRKAB1 and PRKAB2. γ subunit isoforms which are γ1, γ2 and γ3, are expressed by PRKAG1, PRKAG2 and PRKAG3.

These combinations generate 12 possible heterotrimers whose diversity can be increased by post-translational modifications [16], [17]. The heterotrimeric structure of AMPK was shown in Figure 1.8.

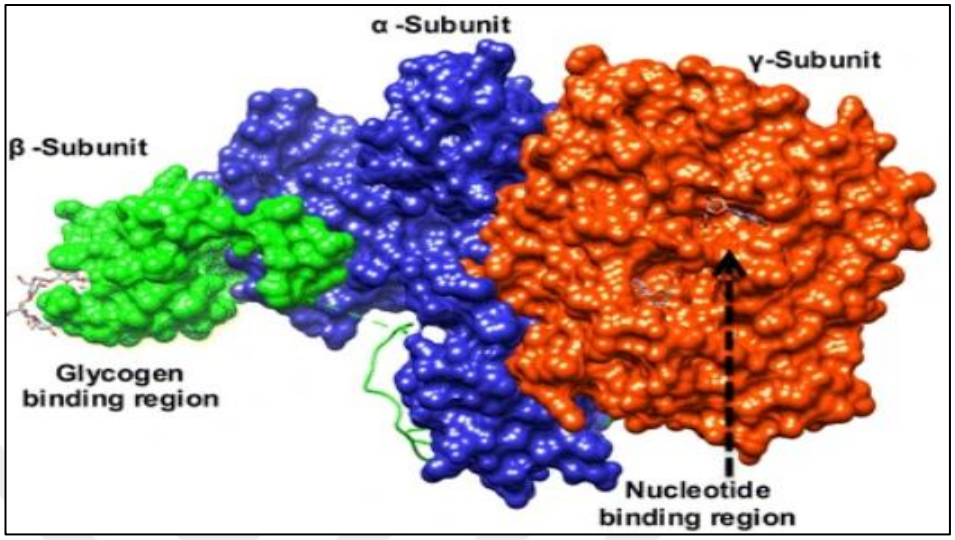

Figure 1. 8: AMPK is a heterotrimeric enzyme which composed of a catalytic subunit (α) with two regulatory subunits (β and γ).

There are stress factors that activates AMPK, which can be classified as canonical and non-canonical. Firstly, as canonical, if cellular AMP: ATP and/or ADP:ATP ratios increased, AMPK activation is triggered by a complex mechanism, involves phosphorylation at threonine residue on the catalytic α subunit (Thr172). AMPK phosphorylation can be catalyzed by two molecules, such as LKB1 and CAMMK2 [15]. AMPK as an energy balancer molecule, sense the decrease of ATP, which is the basic energy molecule of cells to perform cellular activities such as growth and proliferation [17]. The absence of glucose, because of starvation conditions, increase AMP: ATP or ADP:ATP ratio, eventually AMPK become activated. When bound ATP displaced by AMP or ADP, it causes a conformational change of AMPK, that stimulates allosteric activation. Non-canonical pathways involve, firstly, AMPK activation by glucose starvation, which participate in the lysosomal surface, where mammalian target of rapamycin complex-1 (mTORC1), promotes cell survival and growth, regulates AMPK. Secondly, when Ca+2 levels increased in cells, Thr172 in the catalytic α subunit of AMPK.

Additionally, DNA damaging interventions activated AMPK, during cancer treatments. Finally, AMPK is activated by direct binding of long-chain fatty acyl-CoA esters [17].

AMPK activation is mediated via binding of AMP to γ subunit. It can be mediated by 3 ways. Thr172 of AMPK can be phosphorylated by LKB1, protein phosphatases can inhibit the dephosphorylation of Thr172 and AMPK can be activated allosterically by phosphorylating already phosphorylated Thr172 of AMPK [15].

Additionally, AMPK activation can be performed not only by LKB1 but also Ca+2 / calmodulin dependent protein kinase CAMMK1. AMPK works as a metabolic master switch in cells. It turns the direction of cellular metabolism into catabolic state from anabolic state. Therefore, it is suggested that AMPK activators may help treating energy balance related disorders such as obesity and type 2 diabetes. There are AMPK activator agents such as AICAR, PF-739, MK-8722, metformin, phenformin, berberine, sorafenib and arctigenin. They act to activate AMPK by binding" allosteric drug and metabolite" ADaM site, which is the cleft that is bound only by synthetic chemical instead of natural products. Salicylate is the only one that binds ADaM site, which is a compound made by plants act on hormone signalling infection by pathogens [16].

When AMPK activated either through canonical or non-canonical pathways, it redirects cellular metabolism through increased catabolism and decreased anabolism via recruiting multiple pathways in order to maintain cellular homeostasis. It down-regulates some of the proteins, related with anabolic pathways and up-regulates catabolic pathways. While AMPK activation promotes ATP synthesis, it regulates cell growth and proliferation negatively[16]. The location where AMPK is activated, determine the target molecules that will be phosphorylated. For example, ACC is one of the classical targets of AMPK may not be phosphorylated as a result of DNA damage because ACC is not located in nucleus [17].

1.4.1. Downstream Targets of AMPK

AMPK activation trigger phosphorylation of at least 60 downstream proteins, which will reach hundreds eventually. AMPK is a protein kinase that catalyze protein phosphorylation [15].

First and the most important one is ACC1, which is the isoform of acetyl-CoA carboxylase, famous for being AMPK substrate. ACC1 is phosphorylated and become inactivated by the activation of AMPK as key regulatory enzyme of fatty acid synthesis [15],[18].

AMPK not only inhibits ACC1 via phosphorylation but also FASN, which is fatty acid synthase complex. It means AMPK suppresses fat storage by inhibiting fat synthesis and stimulates lipid catabolism [18].

As previously said, AMPK upregulates the catabolism over anabolism, to promote ATP synthesis by enhancing glucose uptake. There are basic downstream pathways that are regulated by AMPK, such as mitochondrial fission, autophagy, mitophagy, mitochondrial biogenesis, fatty acid oxidation and glycolysis. AMPK triggers of fatty acid consumption into mitochondria through phosphorylation of ACC2, which is another isoform of acetyl-CoA carboxylase [18].

AMPK has a regulatory role in autophagy and mitophagy through phosphorylation of ULK1 or Beclin-1 [18].

AMPK inhibits not only fatty acid production but also protein synthesis, by inactivating TORC1, which is one of the central molecules that promotes the initiation of ribosomal protein synthesis. TORC-1 can be inactivated by 2 distinct ways, such as inhibitory phosphorylation of Raptor subunit and activatory phosphorylation of TSC2[16]. mTOR suppression is considered as beneficial for nutrients recycle for having critical role in protein synthesis and suppression of autophagy to promote cell survival under stress conditions [19].

Additionally, AMPK has significant roles for regulation of cell cycle. Basically, because of ATP or glucose starvation that promotes AMPK activation, cause arrest in the G1 phase of cell cycle by increasing the expression of inhibitory proteins that block the movement of protein kinases that are required to pass S phase [19]. It means AMPK impede the duplication of DNA via preventing the entrance of S phase [15].Besides, phosphorylation of p53 at Ser15 occurs indirectly by AMPK [18].

1.4.2. Drugs and Inhibitors for the Treatment of Prostate Cancer via AMPK Activation

Cell growth and proliferation is inhibited by AMPK activation. Therefore, AMPK activation is one of the most feasible therapeutic approaches for treating cancer. Glucose starvation activates AMPK via increasing AMP: ATP and/or ADP:ATP ratio [14]. There are certain reagents that activates AMPK such as metformin and 5-Aminoimidazole-4-carboxyamide ribonucleoside (AICAR). AICAR is an adenosine analog, which is taken up by adenosine transporters and phosphorylated by adenosine kinase. It generates AICAR monophosphate (ZMP), mimics the action of AMP, which binds to site 3 on the α subunit of AMPK. Although, ZMP is about 50-fold less potent than AMP, AICAR is one of the most popular anti-cancer drugs by activating so efficiently AMPK because ZMP can accumulate to millimolar concentrations in cytoplasm [17], [19], [20].

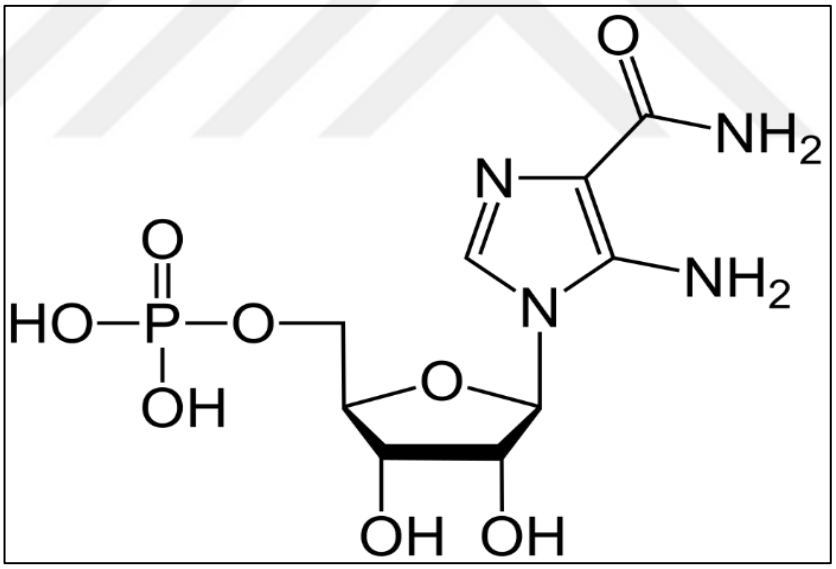

Figure 1. 9: The chemical structure of AICAR, which is an important AMPK activator.

Metformin is another AMPK activator that acts to reduce the rate of glucose production via the activity of 2 key enzymes glucose-6-phosphatase and glucokinase through inactivation of hepatic gluconeogenic genes [21]. Metformin suppresses

gluconeogenesis and enhance glucose uptake. Once AMPK phosphorylated, ACC is inhibited, it causes decrease of lipogenesis and stimulation of fatty acid oxidation [22].

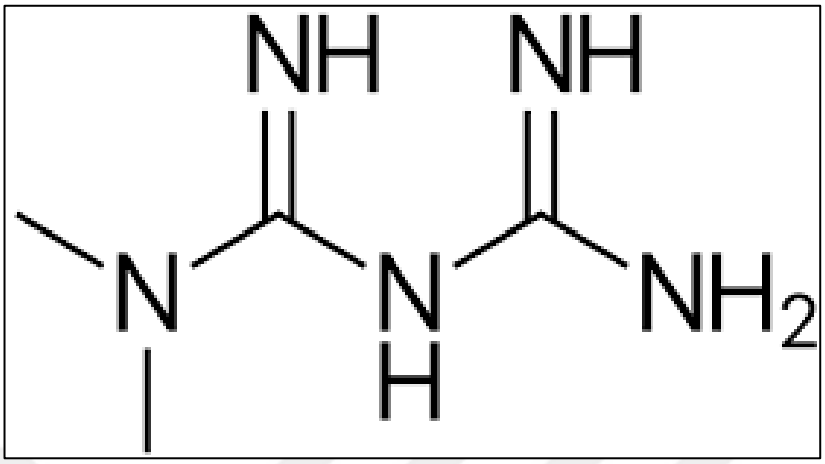

Figure 1. 10: The chemical structure of metformin, which is an important AMPK activator.

Orlistat (tetrahydrolipstatin) is a weight loss agent, which is an inhibitor of pancreatic and other lipases in the lumen, that is used effectively to treat obesity via reduction of absorption of nutrients [23], [24]. It impedes the absorption of nearly one-third of ingested fats. It effects not only weight but also total cholesterol, low density lipoprotein, blood pressure and fasting glucose and insulin concentrations. It shows anti-proliferative effect and induce apoptosis. Additionally, it exerts toxic behavior on cancer cells without any harm on normal cells to suppress tumor growth. Therefore, it is multi-targeted anti-cancer and anti-obesity drug. It acts on FASN to inhibit its activity to suppress lipogenesis. It arrests G2/M phases of cell cycle with dose dependent fashion [23], [25], [26].

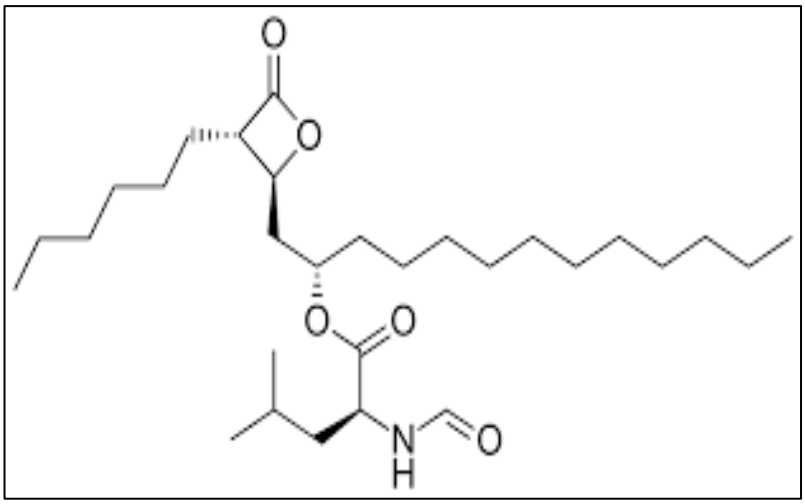

Figure 1. 11: The chemical structure of orlistat, which is an important AMPK activator.

1.5. Aim of the Thesis

Reducing body mass index and body weight in combination with physical activity and diet are the first and most frequently applied methods in the treatment of obesity. Orlistat (Xenical, Roche), is used as anti-obesity drug, approved by the American Food and Pharmaceutical Approval Agency (FDA). It increases the weight loss, regulates body lipid profile and blood pressure. It protects the existing body weight instead of just being effective for losing weight [23], [24].

It was stated from the previous studies that, orlistat induces apoptosis and has anti-proliferative and toxic effects on cancer development without harming to healthy cells, by inhibiting FASN [27].

AMPK regulates cell survival and growth-related pathways and protects ATP levels. ACC, is the substrate of AMPK, is vital for maintaining lipid metabolism and insulin sensitivity. Once AMPK binds and inhibits ACC, it maintains cellular energy homeostasis by regulating apoptosis and autophagy. AMPK activation causes the suppression of prostate cancer cell growth and interferes the mitosis and triggers apoptosis. Therefore, AMPK is shown to be an effective target for the treatment of prostate cancer [14], [19].

The aim of this thesis is to investigate the role of Orlistat as an anti-tumor agent which is a lipase inhibitor used in obesity treatments, on lipogenesis, broken cholesterol metabolism on cancer cells. AMPK α1 mediated effect of orlistat considering AMPK / ULK1 / mTOR signal cascades may provide the identification of protein targets. Eventually, it will gain a novel perspective for the treatment of prostate cancer by clarifying metabolic alterations in the AMPK signalling axis.

2. MATERIALS AND METHODS

2.1. Materials

2.1.1. Laboratory Materials and Equipment

Petri dishes (100 mm) (Lamtek), Tissue culture plates (6-well, 24-well, 60 mm - TRP), tissue culture flasks (T25, T75, T150 - TRP), Falcon tubes (15 mL, 50 mL CAPP), serological pipettes (5 mL, 10 mL ,25 mL - CAPP), Microcentrifuge tubes (1,5 mL, 2mL), Cryotubes (1mL, 2mL), CAPP micropipettes and Expell tips (10µL, 100µL, 1mL)

Micropipettes (Capp), -80°C freezer (VWR), CO_2 incubator (Stericycle i160 - Thermo Scientific), Laminar Flow Cabinet – Safe 2020 (Thermo Scientific), Spectrophotometer – NanoDrop (Shimadzu), Spin (DLab), Vortex (DLab), ZOE Fluorescent Cell Imager (Bio-Rad Laboratories), Heat Block (DLab), Hemocytometer (Marienfeld Improved with Bright Line), 10X Light microscope (used for Cell counting), Water Bath (JeioTech), Transblot Transfer Casette, -20°C freezer, +4°C freezer.

2.1.2. Bacterial Materials

Luria-Bertani Agar (Bioshop), Luria-Bertani Broth Lennox (Bioshop) Cat no: LBL405, Ampicillin (Biomatik), Incubator Shaker (Edmund Bühler), Plasmid isolation kit (EcoSpin Plasmid DNA Isolation Kit, EcoTech Biotechnology). Table 2.1 shows bacterial materials and consumables that were used during the study.

Table 2. 1: Bacterial materials and consumables that were used during thesis.

Material Name	Company	Lot No/Cat no
Luria-Bertani Agar	BioShop	0L67747/ LBL406.1
Luria-Bertani Broth Lennox	BioShop	0K67307/ LBL405.1
Ampicillin	BioShop	0C65047/ AMP201.25
Plasmid DNA Isolation Kit	EcoTech Biotechnology	
Glycerin 85%	Isolab	LR0690709AJW

2.1.3. Material, Equipment and Devices

Materials, equipment and devices that were used during this thesis was shown in Table 2.2.

Table 2. 2: Cell culture consumable materials, used during thesis study, were shown.

Material Name	Company	Lot No/ Cat No:
T25 Cell Culture Plate	TPP	20190430
24 wells plate	TPP	20200272
96 wells plate	TPP	20200240
6 wells plate	TPP	20210260
15 mL centrifuge tubes	CAPP	15CE174B
50 mL centrifuge tubes	CAPP	50C2G1128B
1.5 mL centrifuge tubes	Isolab	MTPPN21015003
2 mL centrifuge tubes	Microcult	270621
1000 µL tip	CAPP/ Expell	P-230724
200 µL tip	CAPP/Expell	P-198179
10 µL tip	Isolab	PTPPI21001002
0,22 µm syringe filter	GVS	7101451
0,45 µm syringe filter	GVS	7091543
Cryotube	Microcult	190321

Equipment and devices that were used during the thesis study was shown in Table 2.3.

Table 2. 3: Equipment and devices used during this thesis was shown in table.

CO2 Incubator	Stericycle i160 Thermo Scientific
Laminar Flow Cabinet	Safe 2020 Thermo Scientific
1000 µL pipet	DLab
200 µL pipet	DLab
10 µL pipet	DLab
Spectrophotometer-NanoDrop	Schimadzu
Spin (Sprout)	DLab
UV illuminator	Vilber Lourmat
Vortex	DLab
ZOE Fluorescent Cell Imager	Bio-Rad Laboratories
Heat Block	DLab
Hemocytometer	Marienfeld
Water Bath	Electromag M24K
Heraeus Hera Safe HS 12 Sterile Cabinet	Kendro Laboratory Products
FLUOstar Omega	BMG LABTECH

2.1.4. Plasmid and Transfection Reagent

Transfection was done with IN-Fect transfection reagent. Expression plasmid LentiCRISPR v2- sg AMPK alpha1 clone3 mammalian expression plasmid (Addgene plasmid # 162121) was purchased from Addgene. The full sequence map for LentiCRISPR v2- sg AMPK alpha1 clone3 mammalian expression plasmid was shown in Figure 2.1.

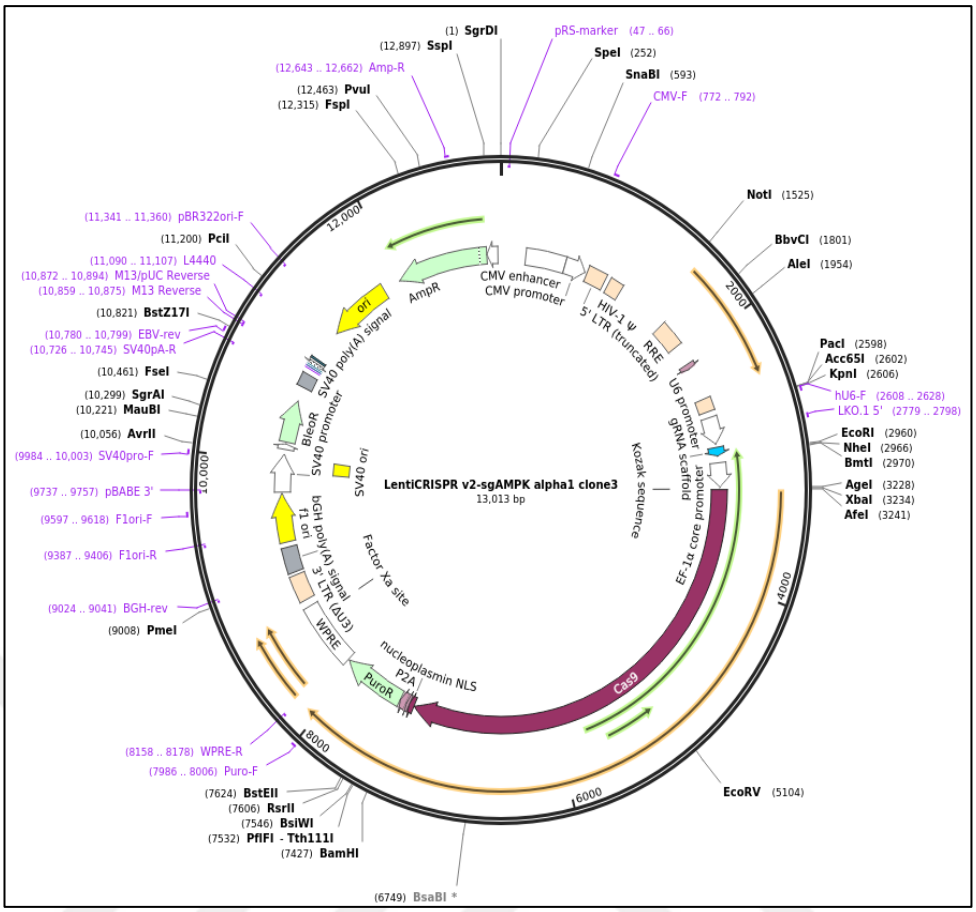

Figure 2. 1: The full sequence map for LentiCRISPR v2- sg AMPK alpha1 clone 3 mammalian expression plasmid (Addgene plasmid # 162121).

2.1.5. Cell Line and Culture Consumables

In this thesis, two different cell lines PC3 (Prostate cancer) ID: CRL-1435 and LNCaP (Lymph Node Carcinoma of the Prostate) CRL-1740 were used (gift from Prof. Dr. Dilek Telci Temeltaş from Yeditepe University).

Roswell Park Memorial Institute (RPMI 1640) 1X with L-glutamine and 4,5g/L Glucose, Fetal Bovine Serum (FBS) (Gibco), Dulbecco's Phosphate Buffered Saline 1X (DPBS) (EcoTech), 0.05% Trypsin-EDTA Solution 1X (Pan Biotech), Penicillin + Streptomycin (10000U-mL Penicillin, 10mg/mL Streptomycin (PAN Biotech), Dimethyl sulfoxide (DMSO). Cell culture consumables were shown in Table 2.4.

Table 2. 4: Cell Culture Consumables that were used in the laboratory.

Name of Material	Company	Cat no/ Lot no:
NutriCulture RPMI 1640	EcoTech Biotechnology	RPMI500/ RP211049
Standard Fetal Bovine Serum (FBS)	PanBiotech	P30-3306
Penicillin, Streptomycin(10000U-mL) Penicillin, 10 mg/mL Streptomycin	PanBiotech	P06-07100/3080821
Trypsin/EDTA	PanBiotech	P10-019100
Dulbecco's Phosphate Buffer Saline 1X (DPBS) pH: 7.4	EcoTech Biotechnology	PBS1X-500/
Dimethyl Sulfoxide (DMSO)	BioFroxx	1084ML100
iNfect^{TM} Transfection Reagent	iNtRON Biotechnology	15081
Puromycin	Invivogen	
MTT	BioFroxx	60D46F07

2.1.6. Protein Isolation and Analysis Materials

Protein isolation and western blot reagents were listed below as Table 2.5.

Table 2. 5: Protein isolation and western blot reagents that were used in the thesis.

M-PER^{TM} Mammalian Protein Extraction Reagent	Thermo SCIENTIFIC	VI311347
Bradford Reagent	Clear Band	BR05/BR0422
Trans-4-Hydroxycinnamic acid	Alfa Aesar	10221426
Luminol	PanReac Applichem	0P009896
Milk Powder	BioFroxx	5E81FA7E

2.2. Methods

2.2.1. Plasmid DNA Isolation

LentiCRISPR v2- sg AMPK alpha1 clone3 mammalian expression plasmid was inoculated Amp+ LB Agar plates, from agar stab overnight.

For miniprep, single colonies were picked from the plate, and they were inoculated in 5 mL Amp+ LB Broth to be used in plasmid DNA isolation, by Ecotech Plasmid DNA Isolation Kit Cat no: EcoPI-50x. Bacterial culture was harvested by centrifugation at 6000 rpm in centrifuge for 2 min at room temperature. Supernatant was discarded using a micropipette. Bacterial pellet was resuspended in 250 µl EcoSpin Resuspension Buffer by vortexing or pipetting up and down until no cell clumps remain. 20 µl of EcoSpin RNAse A to the resuspended mixture. 250 µl of EcoSpin Lysis Buffer was added and mixed gently by inverting the tube 6-7 times. It was incubated at room temperature for 3 min. 350 µl of EcoSpin Binding Buffer was added and mixed thoroughly by inverting the tube 6-7 times. In those stages, the mixture must not be vortexed in order to avoid shearing of genomic DNA. Then it was centrifugated for 5 min at maximum speed at room temperature. An EcoSpin Column was inserted into a collection tube and the supernatant was transferred into the column from the previous stage. It was centrifugated for 30 seconds at room temperature. The flowthrough was discarded and 400 µl of EcoSpin Wash Buffer 1 was added to the EcoSpin Column. It was centrifugated at maximum speed for 30 seconds at room temperature. The flowthrough was discarded and 500 µl of EcoSpin Wash Buffer 2 was added to the Ecospin Column. It was centrifugated at maximum speed for 2 min to completely remove any residual wash buffer. The EcoSpin Column was transferred to a clean 1,5 µl microcentrifuge tube. 30-50 µl of EcoSpin Elution Buffer was added to the center of the column membrane and it was incubated at room temperature for 5 min. It was centrifugated at maximum speed for 30 seconds at room temperature. EcoSpin Column was discarded. Purified DNA concentration was measured by photometric measurements.

2.2.2. Cell Culture

PC3 (ATCC CRL-1435) and LNCaP (ATCC CRL-1740) Prostate cancer cell lines were maintained in Roswell Park Memorial Institute 1640 Medium (RPMI1640) with 10% FBS and 1% Penicillin Streptomycin in 37°C and 5% CO_2. After the cells removed from the -80°C, they were placed at 37°C and 5% CO_2 to equilibrate temperature and carbon dioxide. After the frozen cells were thawed, the cells were transferred to cell culture dish and left for incubation.

After fourth hour of incubation, whole medium was taken, and fresh media was added. After the cell density reached 80%, cells were trypsinized and collected and. They were passaged into two separate T25 cell culture dishes to proliferate.

When, the cell density reached 80%, they were collected with trypsin and counted by Hemocytometer (Marienfield).

Before use, the Hemocytometer glass was cleaned with 70% alcohol. In the cell suspension, 10 microliters are taken with a micropipette and placed on the hematocytometer glass and covered with coverslip. This preparation was examined in 10X microscope. Cells in 16 squares in the corners were counted, averaged, and multiplied by 10.000 for 1 mL of cell suspension.

2.2.3. Cell Transfection for AMPK $^{-/-}$ Cell generation

Knockout of AMPKα1 in PC3 (ATCC CRL-1435) and LNCaP (ATCC CRL-1740) cell lines were performed using single guide RNA (sgRNA) and CRISPR/Cas9 technology. LentiCRISPR v2-sgAMPK alpha1 clone 3 was obtained from Addgene.

250.000 of PC3 cells were seeded in 6 wells plate and incubated for a day in 37 °C and 5% CO_2 in incubator. Then, 2 ug of plasmid and 3 µl of IN-fect^{TM} Transfection reagent were prepared in Serum-free RPMI and added to the cells at 2:3 ratio and incubate for 48 hours. After 4 hours of transfection, 1 mL 20% FBS RPMI was added to the wells. After 48 hours of transfection, the medium in the petri dish was discarded, and the medium containing 200 ng of Puromycin, which is the antibiotic suitable for this plasmid, was added in the petri dish and incubated in the incubator for 3 days. Then, the medium containing 200 ng Puromycin was discarded and the medium containing 400 ng of puromycin was added.

The concentration of puromycin was increased gradually, as 800 ng, 1000ng, 1200ng, 1500 ng and 2000 ng for 3 days in order to select transfected cells over non-transfected ones. Cell density and cytotoxicity were examined.

After determining the optimum Puromycin dose for the cells to be selected, stable colonies and the cells in this colony were seeded into 96 wells plate for single cell generation. Selected single cells were waited for 1-3 weeks in order for them to grow.

The grown single cell-generated cells were transferred into a T25 petri dish and their growth was ensured. Protein isolation was made from the obtained cells and the level of AMPK protein was checked by western blotting (WB).

250.000 of LNCaP cells were seeded in 6 wells plate and incubated for a day in 37 °C and 5% CO_2 in incubator. Then, 1 ug of plasmid and 6 µl of IN-fect™ Transfection reagent were prepared in Serum-free RPMI and added to the cells at 2:3 ratio and incubate for 48 hours. After 4 hours of transfection, 1 mL 20% FBS RPMI was added to the wells.

After 48 hours of transfection, the medium in the petri dish was discarded, and the medium containing 200 ng of Puromycin, which is the antibiotic suitable for this plasmid, was added in the petri dish and incubated in the incubator for 3 days. Then, the medium containing 200 ng Puromycin was discarded and the medium containing 400 ng of puromycin was added. The concentration of puromycin was increased gradually, as 800 ng,1000ng,1200ng,1500 ng and 2000 ng for 3 days in order to select transfected cells over non-transfected ones. Cell density and cytotoxicity were examined. After determining the optimum Puromycin dose for the cells to be selected, stable colonies and the cells in this colony were seeded into 96 wells plate for single cell generation. Selected single cells were waited for 1-3 weeks in order for them to grow.

The grown single cell-generated cells were transferred into a T25 petri dish, and their growth was ensured. Protein isolation was made from the obtained cells and the level of AMPK protein was checked by western blotting (WB).

2.2.4. Dose Dependent Cellular Viability Test (MTT)

The Prostate cancer cells PC3 and LNCaP were seeded at $1x10^4$ cells/well into the 96 wells petri dish, and then incubated overnight in a 37 °C and 5% CO_2 incubator for adherence. Then, 0-100 μM Orlistat was applied to the cells. They were incubated at 37 °C and 5% CO_2 incubator for adherence. At the end of 24h, 10μl of MTT reagent was added to the medium on the cells. The samples were kept in incubator at 37 °C and 5% CO_2 for 4 hours.

After 4 hours, all the medium was discarded and 100 μl of DMSO was added to each well and incubated in the dark on shaker for 15 mins for the formazan crystals to dissolved. Absorbance was measured at two wavelengths at 570 nm in Omega Microplate Reader.

2.2.5. DIOC6 and PI Staining

The Prostate cancer cells PC3 and LNCaP were seeded at $5x10^4$ cells/well into the 24 wells petri dish, and then incubated 24 h in a 37 °C and 5% CO_2 incubator for adherence. Selected dosages of Orlistat were applied to adherent cells.

After 24h, the media of the cells were replaced with media containing 4nM DIOC6 incubated for 15 min. Living cells were selected by staining the healthy mitochondrial membrane. Cells with healthy mitochondrial membranes were visualized as green at 488 nm excitation and 525 nm emission at the end of 15 minutes under fluorescence microscope.

2.2.6. Colony Formation Assay

The prostate cancer cells PC3 and LNCaP were seeded in a 6 wells plate as $2,5x10^3$ cells and incubated overnight in a a 37 °C and 5% CO_2 incubator for adherence. Selected dosages of Orlistat were applied to adherent cells. After 24h of drug application, cells were exchanged with complete media. After 10-14 days, the media was discarded, and wells were washed with 1X PBS and incubated with 3 mL of 100% methanol and 1 mL of acetic acid for 5 min. After fixation, cells were stained with crystal violet and the colony formation potential was visualized.

2.2.7. BODIPY Staining

The Prostate cancer cells PC3 and LNCaP were seeded at $5x10^4$ cells/well into the 24 wells petri dish, and then incubated 24 h in a 37 °C and 5% CO_2 incubator for adherence. Selected dosages of Orlistat were applied to adherent cells.

After 24h, the media of the cells were replaced with media containing 1:1000 BODIPY stain, incubated for 15 min.

Cells with lipid droplets were visualized as green at 488 nm excitation and 525 nm emission at the end of 15 minutes under fluorescence microscope.

2.2.8. Total Protein Isolation

Prostate cancer cells PC3 and LNCaP were seeded in 6 wells plate as $2,5x10^3$ cells and incubated overnight in a 37 °C and 5% CO2 incubator for adherence. Selected dosages of Orlistat were applied to adherent cells.

After 24h of drug application, cells were collected from the petri dish by scraping using 1X PBS solution and precipitated by centrifugation at 13200 rpm for 2 min. Supernatant was discarded. 30-80 µl of M-PER™ Mammalian Protein Extraction Reagent was added to the cell pellet to be dissolved. The samples were incubated in a shaker for 20 min at +4°C to be centrifugated at 13200 rpm for 15 min. The supernatant was taken into a fresh eppendorf tube and stored at -20°C.

2.2.9. Determination of Protein Concentration with Bradford Assay

The Bradford Assay was used to determine the protein concentration. Firstly, a standard curve was created by using increasing amounts of Bovine Serum albumin (BSA) with a concentration of 1,5 ug/ul, 3ug/ul, 4.5ug/ul, 6ug/µl and 7.5 ug/µl BSA. 1µl of each sample was added into 96 wells plate and 100 µl of Bradford reagent was added. It was incubated at shaker in the dark for 5 min. The absorbances of samples were read in a microplate reader at 595 nm wavelength. Protein concentration values were calculated by the resulting absorbance values.

2.2.10. Western Blotting (Immunoblotting)

Proteins whose concentrations were calculated by Bradford Assay, were mixed with Laemmli (4X) loading buffer and 30-50 ug of protein samples at a ratio of 1:4 and incubated at 70°C for 10 minutes. Prepared proteins were loaded on 12% Acrylamide/bisacrylamide gel at the determined concentrations and run at 80-120V in a tank with running buffer. Polyvinyl fluoride (PVDF) membranes to be used were activated with methanol before the executed proteins were transferred.

The proteins in the gel were transferred to the membrane by the TransBlot machine at 2.5mA for 30 minutes. After the transfer process, the membrane was blocked with 5% skim milk powder (1X TBS containing 0.1% Tween 20) at room temperature for 1 hour in the shaker at room temperature. After blocking process, membrane was incubated with selected primary antibody (1:1000 in TBS-T solution) overnight in +4°C. Then, membrane was washed three times with TBS-T solution. The membrane was incubated with the secondary antibody at room temperature for 1 hour. The membrane was washed 2 times with TBS-T and 1 time with TBS. Band imaging of antibody bound proteins in the membrane was performed using ChemiDoc. The bands of control and treated samples were analyzed by ImageJ.

2.2.12. Statistical Analysis

The results for the impact of MTT cell viability assay were analyzed using statistical methods compatible with the amount of data via MS-Office Excel 2010. Student t-test was utilized by two tailed paired t-test. $p<0.05$ was taken as a level of significance.

The results for the impact of immunoblotting were analyzed using Image J program, each sample was measure via single replicate [28].

3. RESULTS

3.1. PC3 and LNCaP Prostate Cancer Cells Transfection Optimizations

Firstly, transfection reagent was optimized for PC3 prostate cancer cell, by applying 1:3 and 1:6 transfection ratio by transfecting GFP tagged plasmid. Figure 3.1 shows the transfection efficiency of iNfect transfection reagent on PC3 cell lines for 24 h.

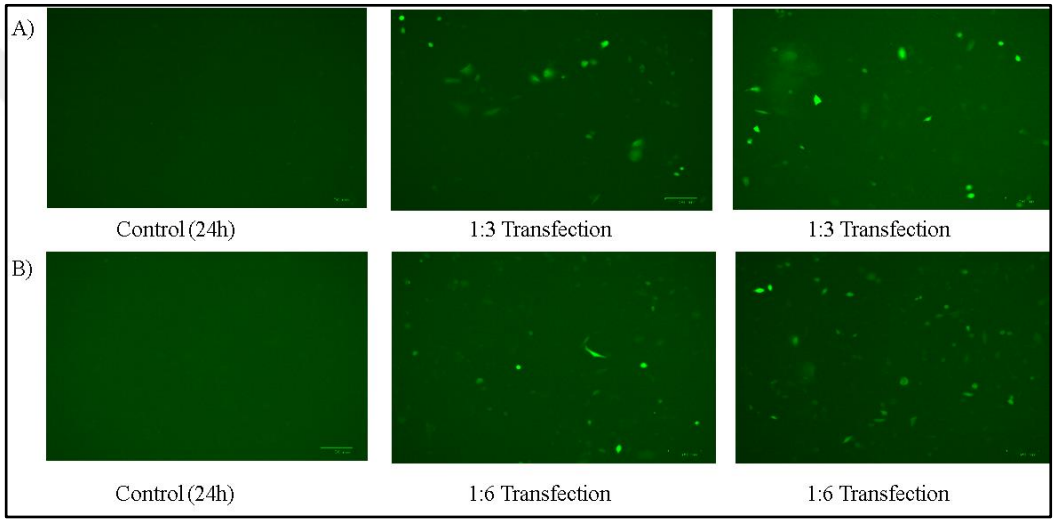

Figure 3. 1 Transfection reagent optimization on PC3 prostate cancer cells for 24 h. a) $2.5x10^5$ cells were seeded and 1:3 transfection ratios were applied. b) $2.5x10^5$ cells were seeded and 1:6 transfection ratios were applied. Fluorescence intensity of cells that were transfected with GFP tagged plasmids were compared.

After 48 hours of transfection, cells were visualized by ZOE fluorescent microscope to observe transfection efficiency to decide which transfection ratio is the most effective one. Figure 3.2 shows the transfection efficiency of iNfect transfection reagent on PC3 cell lines for 48 h.

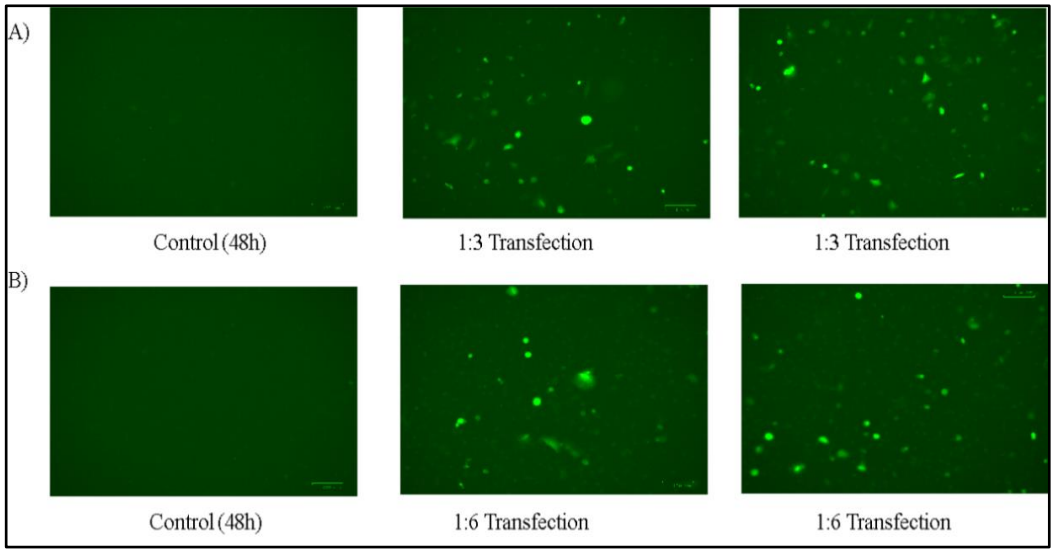

Figure 3. 2: Transfection reagent optimization on PC3 prostate cancer cells for 48 h. a) $2.5x10^5$ cells were seeded and 1:3 transfection ratios were applied. b) $2.5x10^5$ cells were seeded and 1:6 transfection ratios were applied. Fluorescence intensity of cells that were transfected with GFP tagged plasmids were compared.

1:3 ratio of transfection on PC3 prostate cancer cells was determined for CRISPR/Cas9 mediated AMPK $^{-/-}$ cell generation procedure.

After that, transfection reagent for LNCaP prostate cancer cells was optimized by 1:3 and 1:6 transfection ratio by fluorescent microscope ZOE. Figure 3.3 shows the transfection efficiency of transfection reagent on LNCaP cell lines for 24 h.

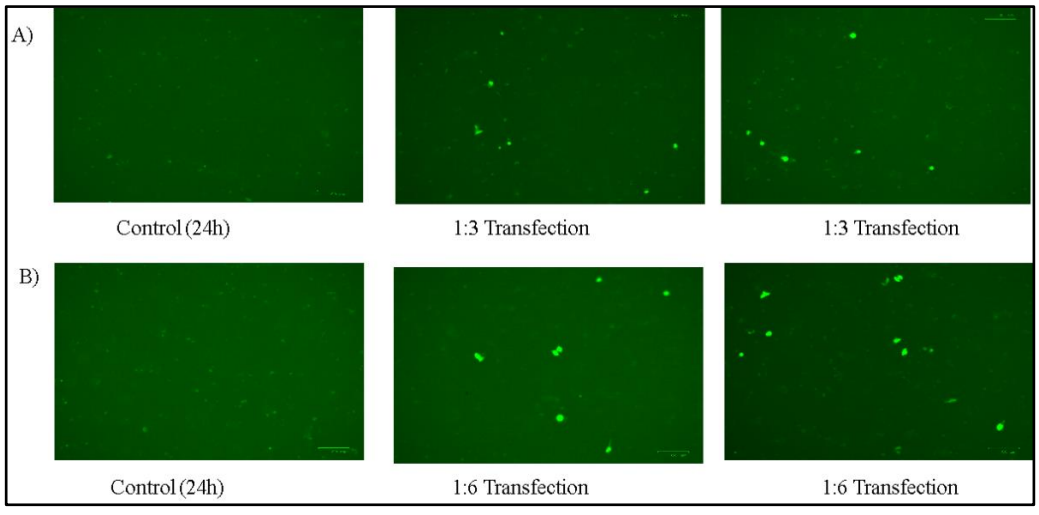

Figure 3. 3: Transfection reagent optimization on LNCaP prostate cancer cells for 24 h. a) $2.5x10^5$ cells seeded and 1:3 transfection ratios were applied. b) $2.5x10^5$ cells seeded and 1:6 transfection ratios were applied. Fluorescence intensity of cells that were transfected with GFP tagged plasmids were compared.

After 48 hours of transfection, cells were visualized with ZOE fluorescent microscope to observe transfection efficiency and decide which transfection ratio is the most effective one. Figure 3.4 shows the transfection efficiency of transfection reagent on LNCaP cell lines for 48 h.

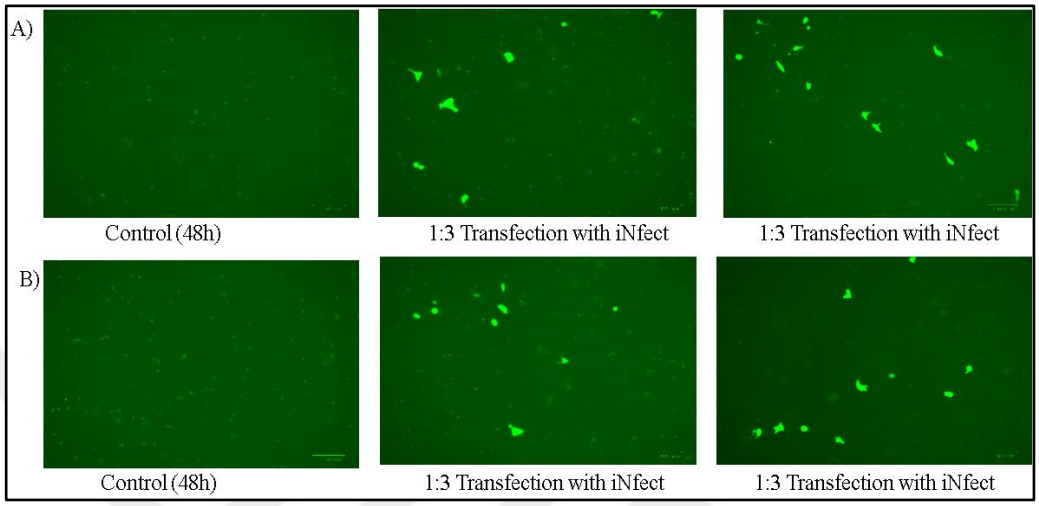

Figure 3. 4: Transfection reagent optimization on LNCaP prostate cancer cells for 48 h. a) $2.5x10^5$ cells seeded and 1:3 transfection ratios were applied. b) $2.5x10^5$ cells seeded and 1:6 transfection ratios were applied. Fluorescence intensity of cells that were transfected with GFP tagged plasmids were compared.

1:6 ratio of transfection on LNCaP prostate cancer cells was determined for CRISPR/Cas9 mediated AMPK $^{-/-}$ cell generation procedure.

3.2. Cell Transfection and Puromycin Selection for PC3 and LNCaP cells

After 48 h of transfection on PC3 and LNCaP prostate cancer cells, transfected cells were selected over untransfected ones gradually by puromycin antibiotic, which is the selectable marker of the lentiviral vector, that is used in this study. Figure 3.5 shows 1^{th} day of 800 ng puromycin treatment on PC3 cells.

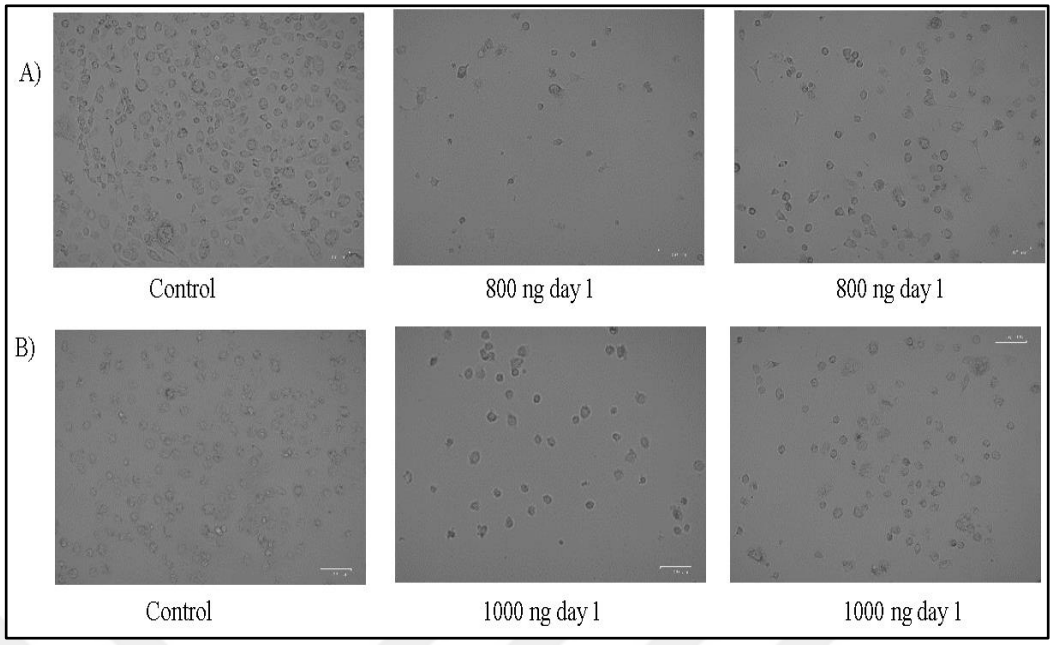

Figure 3. 5: After 48 h of transfection on PC3 prostate cancer cells, transfected cells were selected with selected doses of Puromycin. Controls were maintained with complete RPMI. a) 800 ng of puromycin was applied on 1:3 transfected PC3 cells for 24 h. b) 1000 ng of puromycin was applied on 1:3 transfected PC3 cells for 24 h. Cells were observed by brightfield mode of fluorescence cell imager at 100 nm scale.

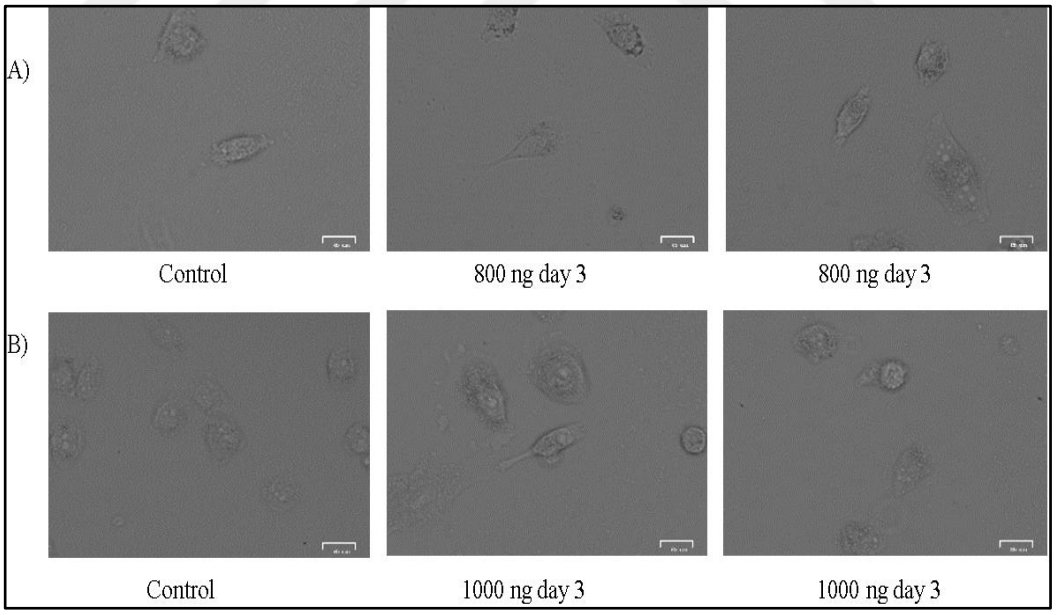

Figure 3. 6: After 48 h of transfection on PC3 prostate cancer cells, transfected cells were selected with selected doses of Puromycin. Controls were maintained with complete RPMI. a) 800 ng of puromycin was applied on 1:3 transfected PC3 cells for 72 h. b) 1000 ng of puromycin was applied on 1:3 transfected PC3 cells for 72 h. Cells were observed by brightfield mode of fluorescence cell imager at 25 nm scale.

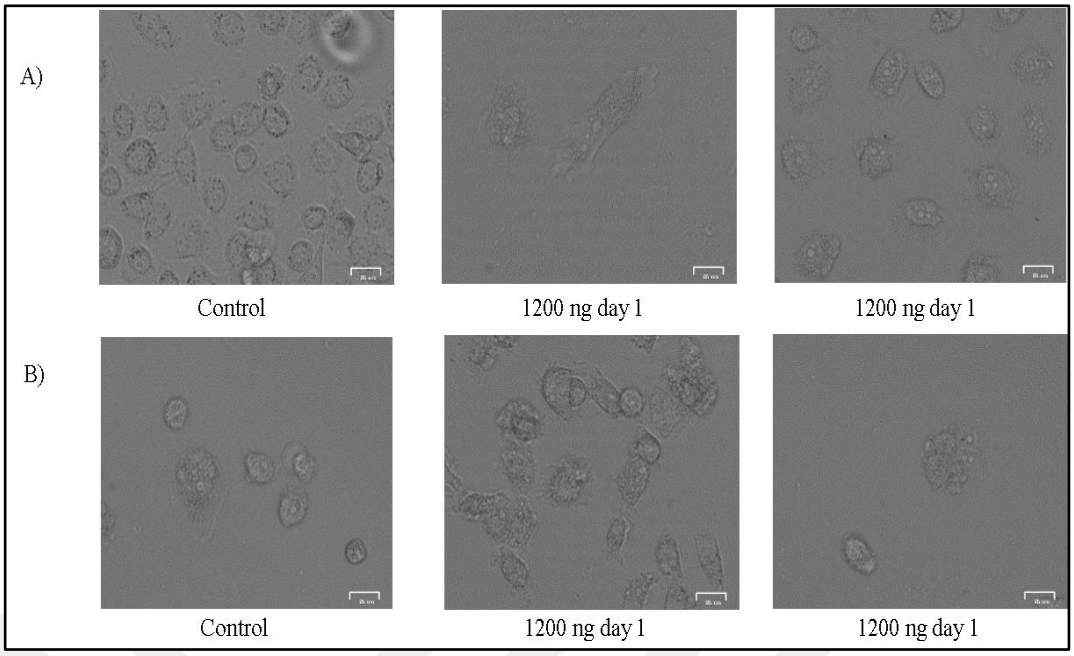

Figure 3. 7: After 48 h of transfection on PC3 prostate cancer cells, transfected cells were selected with selected doses of Puromycin. Controls were maintained with complete RPMI. a) 1200 ng of puromycin was applied on 1:3 transfected PC3 cells for 24 h. b) 1200 ng of puromycin was applied on 1:3 transfected PC3 cells for 24 h. Cells were observed by brightfield mode of fluorescence cell imager at 25 nm scale.

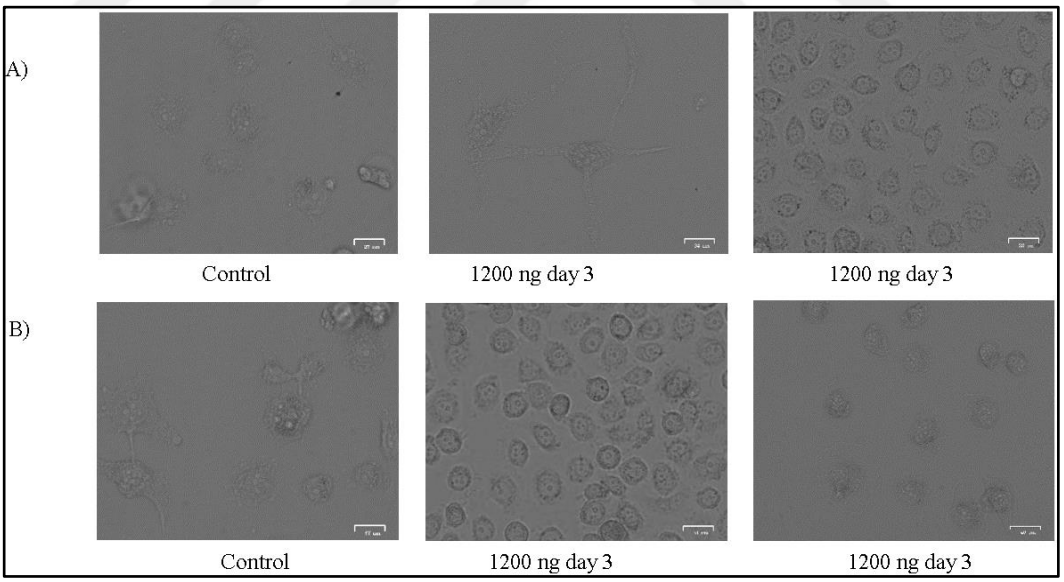

Figure 3. 8: After 48 h of transfection on PC3 prostate cancer cells, transfected cells were selected with selected doses of Puromycin. Controls were maintained with complete RPMI. a) 1200 ng of puromycin was applied on 1:3 transfected PC3 cells for 72 h. b) 1200 ng of puromycin was applied on 1:3 transfected PC3 cells for 72 h. Cells were observed by brightfield mode of fluorescence cell imager at 25 nm scale.

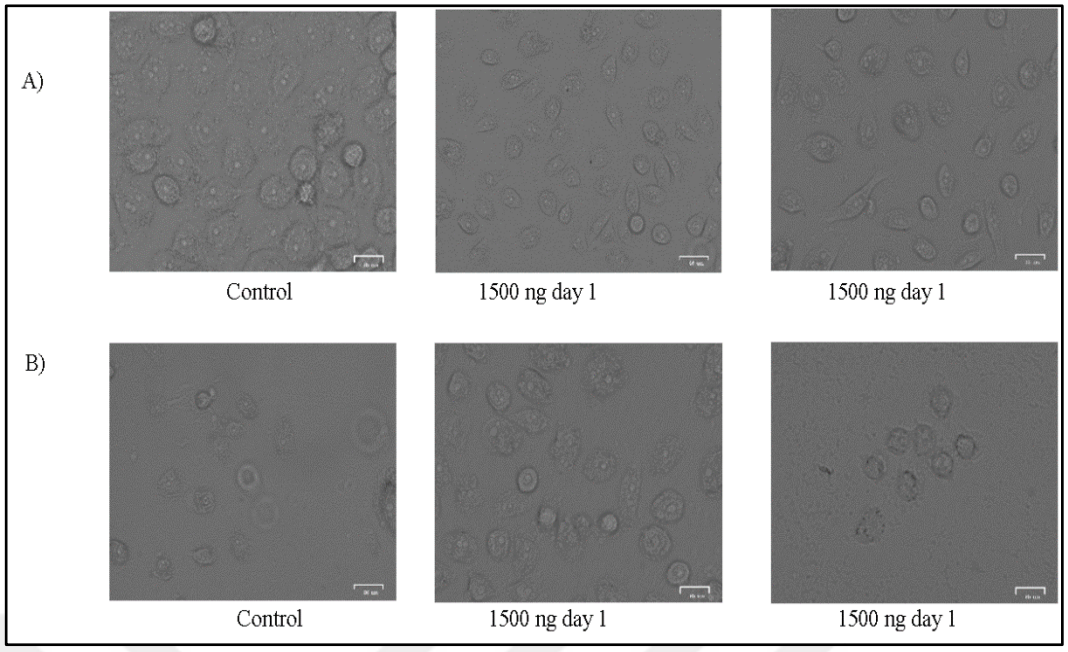

Figure 3. 9: After 48 h of transfection on PC3 prostate cancer cells, transfected cells were selected with selected doses of Puromycin. Controls were maintained with complete RPMI. a) 1500 ng of puromycin was applied on 1:3 transfected PC3 cells for 24 h. b) 1500 ng of puromycin was applied on 1:3 transfected PC3 cells for 24 h. Cells were observed by brightfield mode of fluorescence cell imager at 25 nm scale.

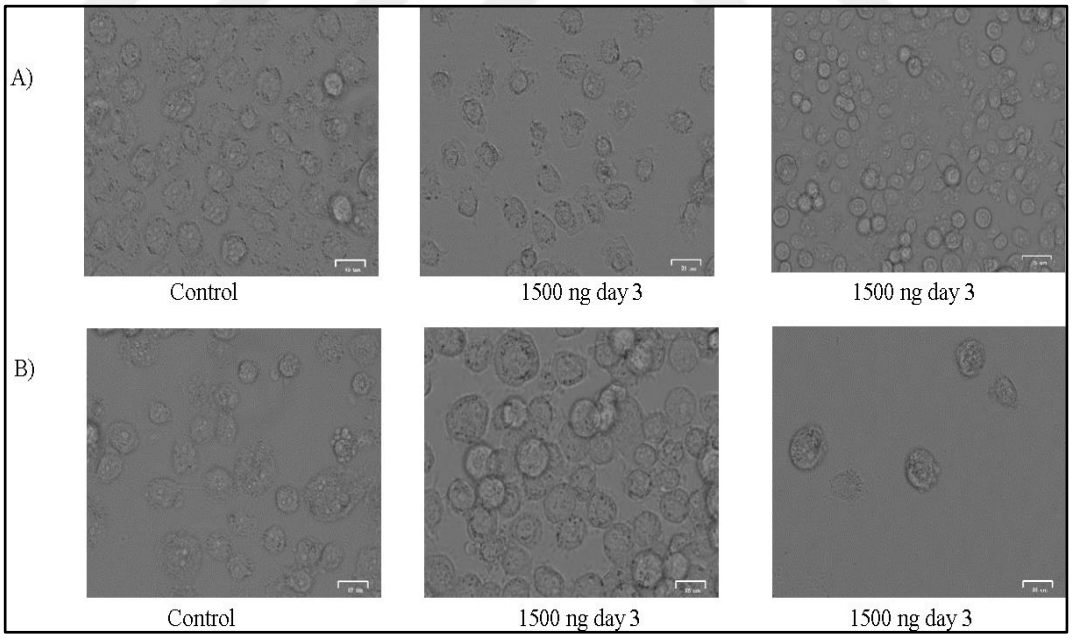

Figure 3. 10: After 48 h of transfection on PC3 prostate cancer cells, transfected cells were selected with selected doses of Puromycin. Controls were maintained with complete RPMI. a) 1500 ng of puromycin was applied on 1:3 transfected PC3 cells for 72 h. b) 1500 ng of puromycin was applied on 1:3 transfected PC3 cells for 72 h. Cells were observed by brightfield mode of fluorescence cell imager at 25 nm scale.

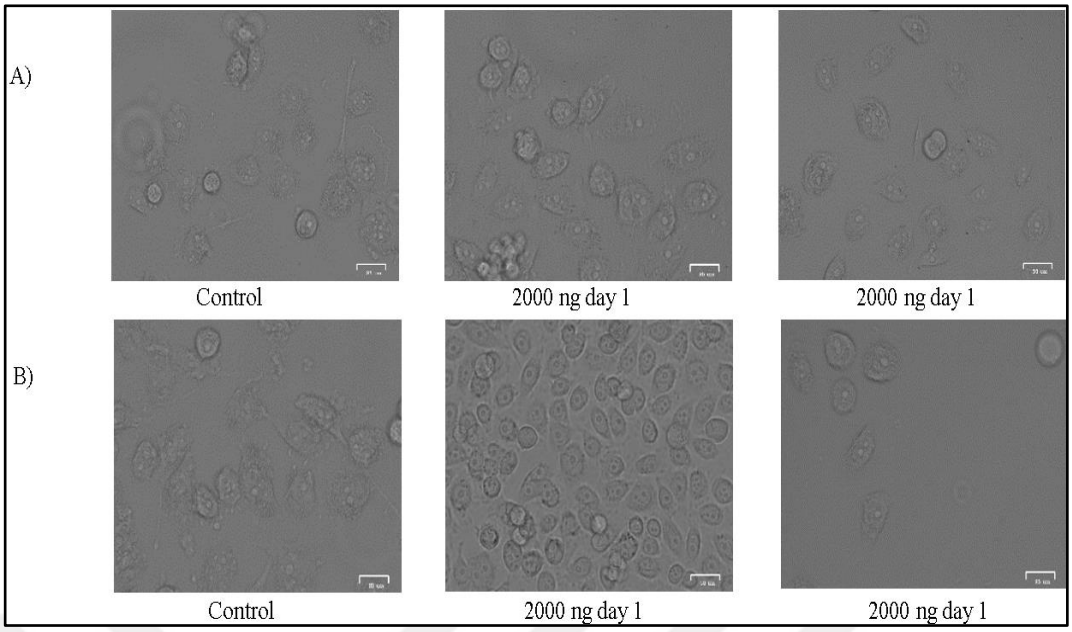

Figure 3. 11: After 48 h of transfection on PC3 prostate cancer cells, transfected cells were selected with selected doses of Puromycin. Controls were maintained with complete RPMI. a) 2000 ng of puromycin was applied on 1:3 transfected PC3 cells for 24 h. b) 2000 ng of puromycin was applied on 1:3 transfected PC3 cells for 24 h. Cells were observed by brightfield mode of fluorescence cell imager at 25 nm scale.

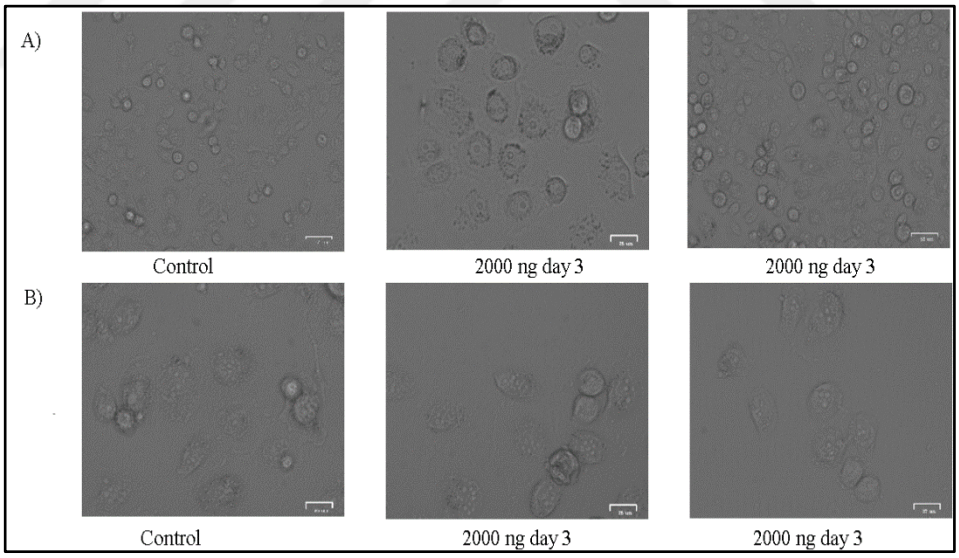

Figure 3. 12: After 48 h of transfection on PC3 prostate cancer cells, transfected cells were selected with selected doses of Puromycin. Controls were maintained with complete RPMI. a) 2000 ng of puromycin was applied on 1:3 transfected PC3 cells for 72 h. b) 2000 ng of puromycin was applied on 1:3 transfected PC3 cells for 72 h. Cells were observed by brightfield mode of fluorescence cell imager at 25 nm scale.

After that, immunoblotting was performed to check the knocking out of AMPK α1. We observed AMPK α1 band on both control (untransfected) and transfected cells. The protein expression result of the PC3 prostate cancer cell was shown in Figure 3.13.

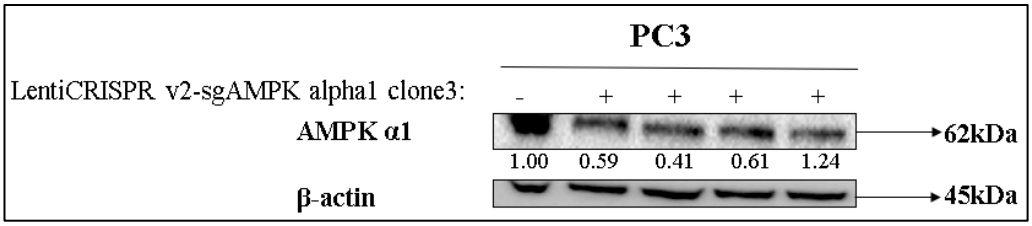

Figure 3. 13: Following the 3 rd day of 2 µg puromycin treatment the total protein isolation of PC3 cells was performed. AMPK α1 protein expression levels of transfected wells and an untransfected well of PC3 prostate cancer cell was shown. β-actin was used as a loading control.

It was observed that AMPK α1 protein expression is carried out despite the transfection, which was mediated by CRISPR/Cas9. Then it was decided to repeat the transfection by increasing the concentration of lentiviral vector's DNA to the cells which were already transfected. After 48 h, we initiated the puromycin selection with 200 ng, which will increase gradually. Figure 3.14 shows the 1st day of 200 ng puromycin treatment on PC3 cells. Figure 3.15-21 shows the gradual increase of puromycin concentration for puromycin selection of PC3 prostate cancer cells.

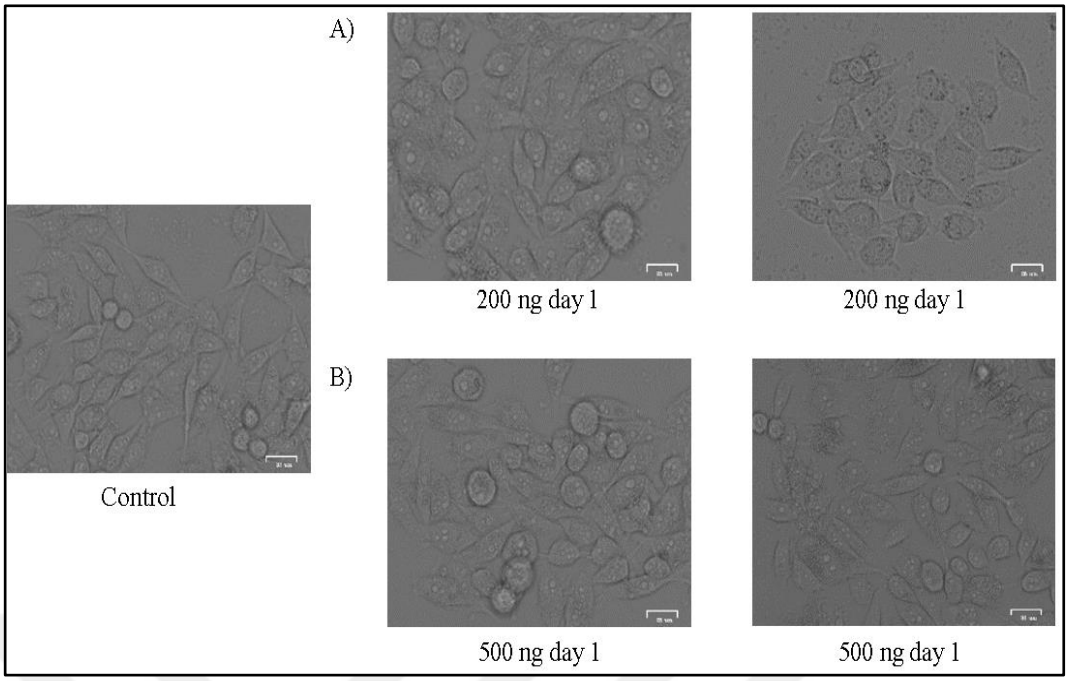

Figure 3. 14: After 48 h of second transfection on PC3 prostate cancer cells, transfected cells were selected with selected doses of Puromycin. Controls were maintained with complete RPMI. a) 200 ng of puromycin was applied on 2:3 transfected PC3 cells for 24 h. b) 500 ng of puromycin was applied on 2:3 transfected PC3 cells for 24 h. Cells were observed by brightfield mode of fluorescence cell imager at 25 nm scale.

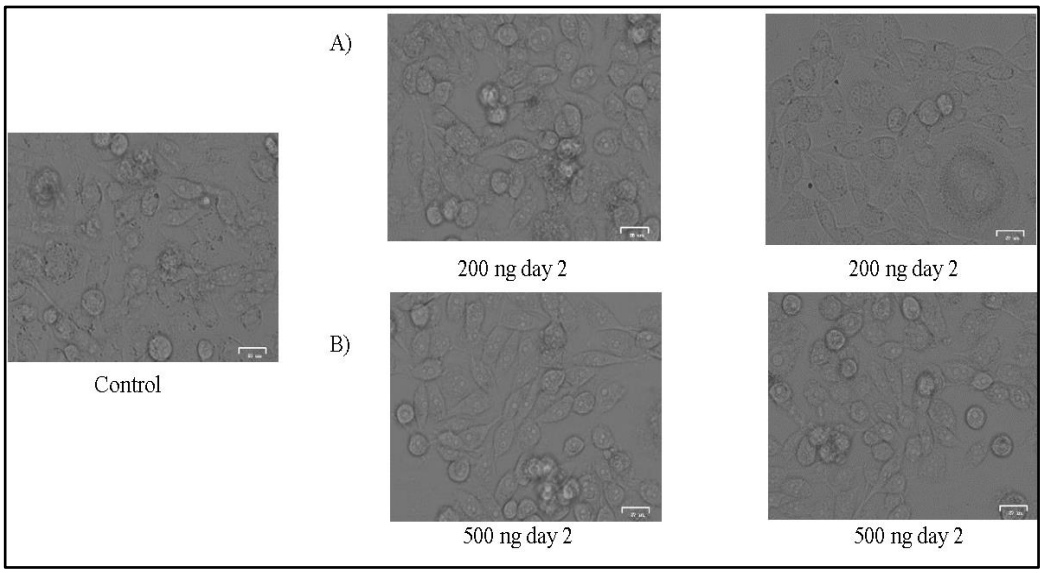

Figure 3. 15: After 48 h of second transfection on PC3 prostate cancer cells, transfected cells were selected with selected doses of Puromycin. Controls were maintained with complete RPMI. a) 200 ng of puromycin was applied on 2:3 transfected PC3 cells for 48 h. b) 500 ng of puromycin was applied on 2:3 transfected PC3 cells for 48 h. Cells were observed by brightfield mode of fluorescence cell imager at 25 nm scale.

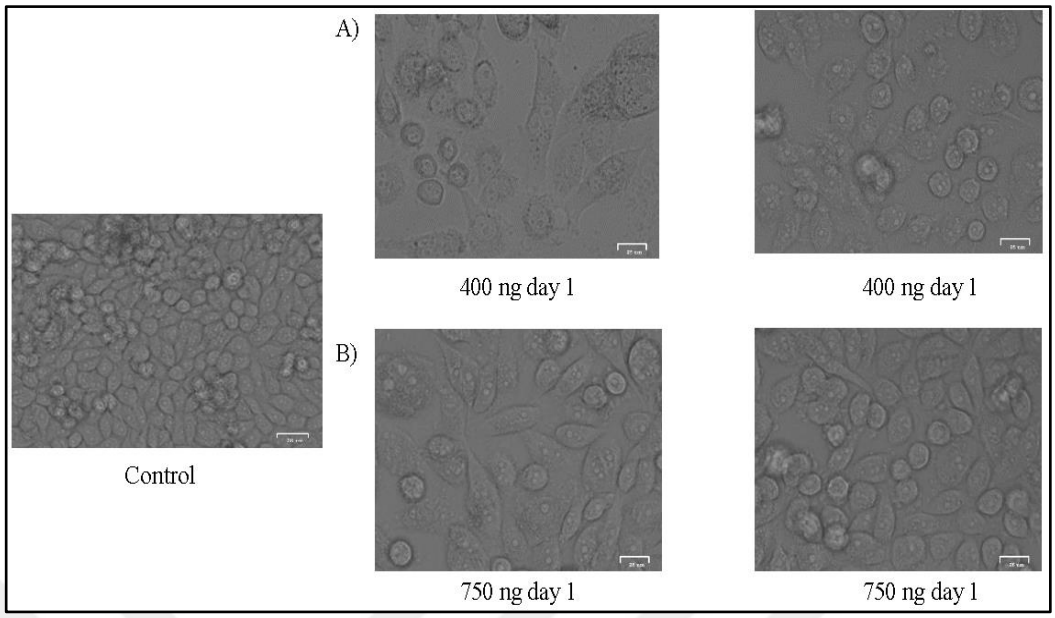

Figure 3. 16: After 48 h of second transfection on PC3 prostate cancer cells, transfected cells were selected with selected doses of Puromycin. Controls were maintained with complete RPMI. a) 400 ng of puromycin was applied on 2:3 transfected PC3 cells for 24 h. b) 750 ng of puromycin was applied on 2:3 transfected PC3 cells for 24 h. Cells were observed by brightfield mode of fluorescence cell imager at 25 nm scale.

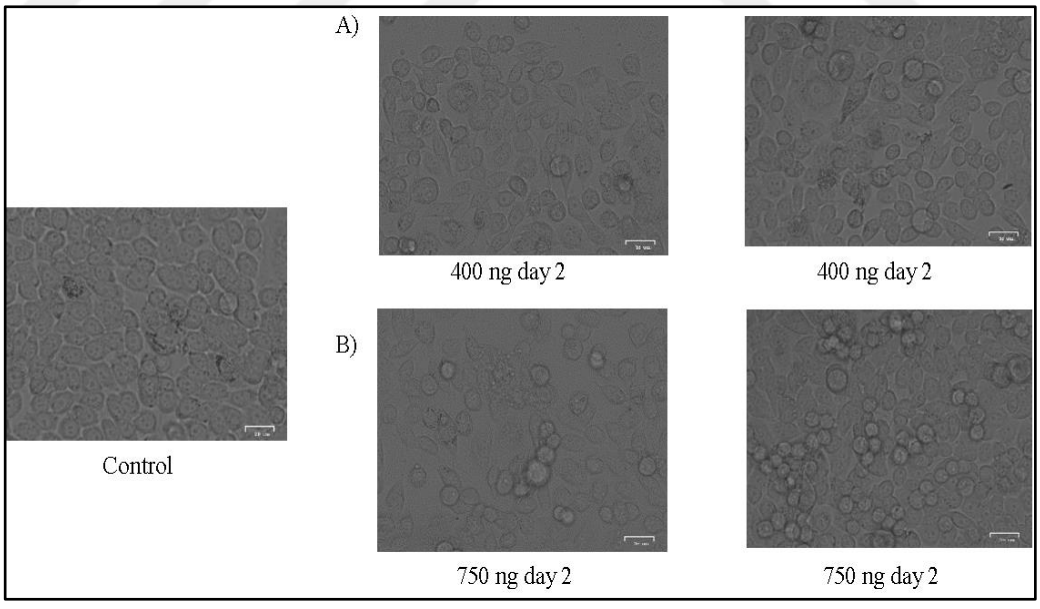

Figure 3. 17: After 48 h of second transfection on PC3 prostate cancer cells, transfected cells were selected with selected doses of Puromycin. Controls were maintained with complete RPMI. a) 400 ng of puromycin was applied on 2:3 transfected PC3 cells for 48 h. b) 750 ng of puromycin was applied on 2:3 transfected PC3 cells for 48 h. Cells were observed by brightfield mode of fluorescence cell imager at 25 nm scale.

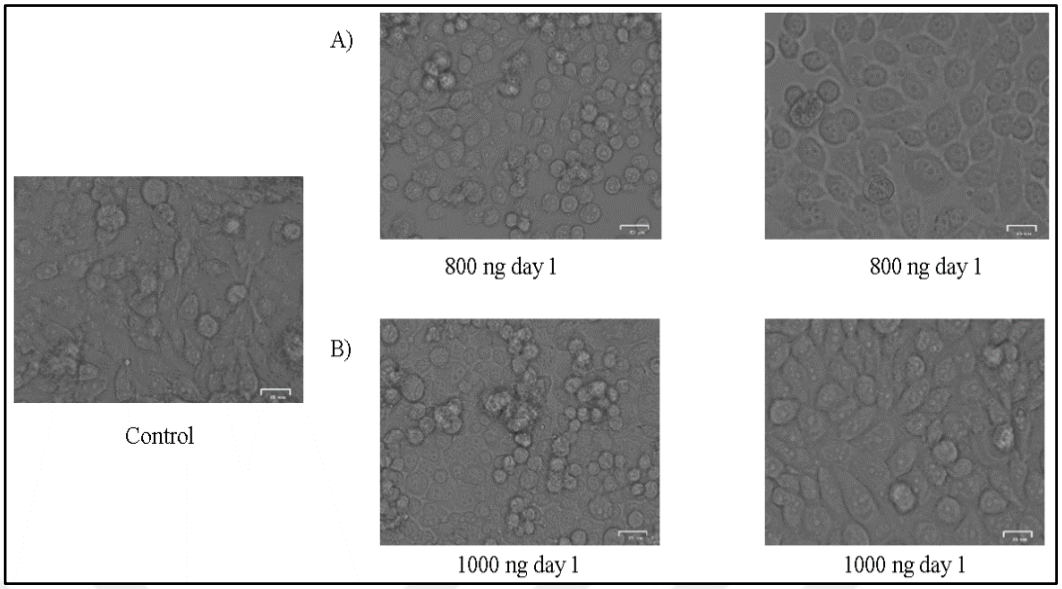

Figure 3. 18: After 48 h of second transfection on PC3 prostate cancer cells, transfected cells were selected with selected doses of Puromycin. Controls were maintained with complete RPMI. a) 800 ng of puromycin was applied on 2:3 transfected PC3 cells for 24 h. b) 1000 ng of puromycin was applied on 2:3 transfected PC3 cells for 24 h. Cells were observed by brightfield mode of fluorescence cell imager at 25 nm scale.

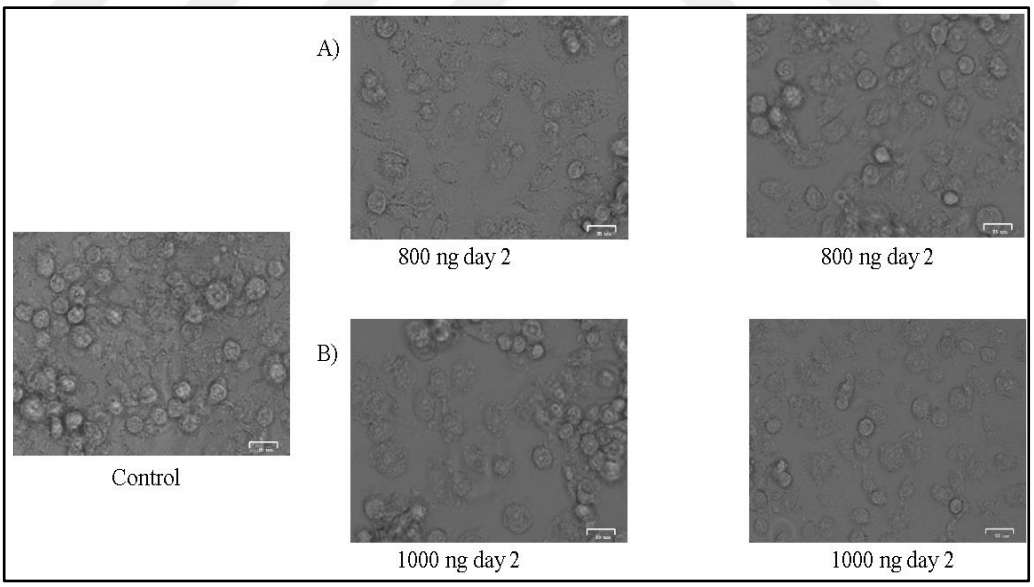

Figure 3. 19: After 48 h of second transfection on PC3 prostate cancer cells, transfected cells were selected with selected doses of Puromycin. Controls were maintained with complete RPMI. a) 800 ng of puromycin was applied on 2:3 transfected PC3 cells for 48 h. b) 1000 ng of puromycin was applied on 2:3 transfected PC3 cells for 48 h. Cells were observed by brightfield mode of fluorescence cell imager at 25 nm scale.

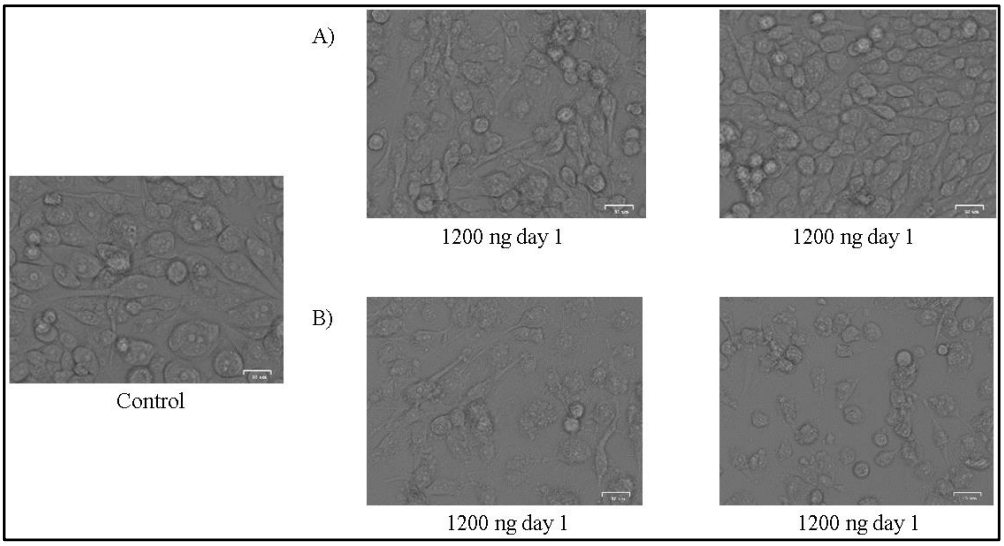

Figure 3. 20: After 48 h of second transfection on PC3 prostate cancer cells, transfected cells were selected with selected doses of Puromycin. Controls were maintained with complete RPMI. a) 1200 ng of puromycin was applied on 2:3 transfected PC3 cells for 24 h. b) 1200 ng of puromycin was applied on 2:3 transfected PC3 cells for 24 h. Cells were observed by brightfield mode of fluorescence cell imager at 25 nm scale.

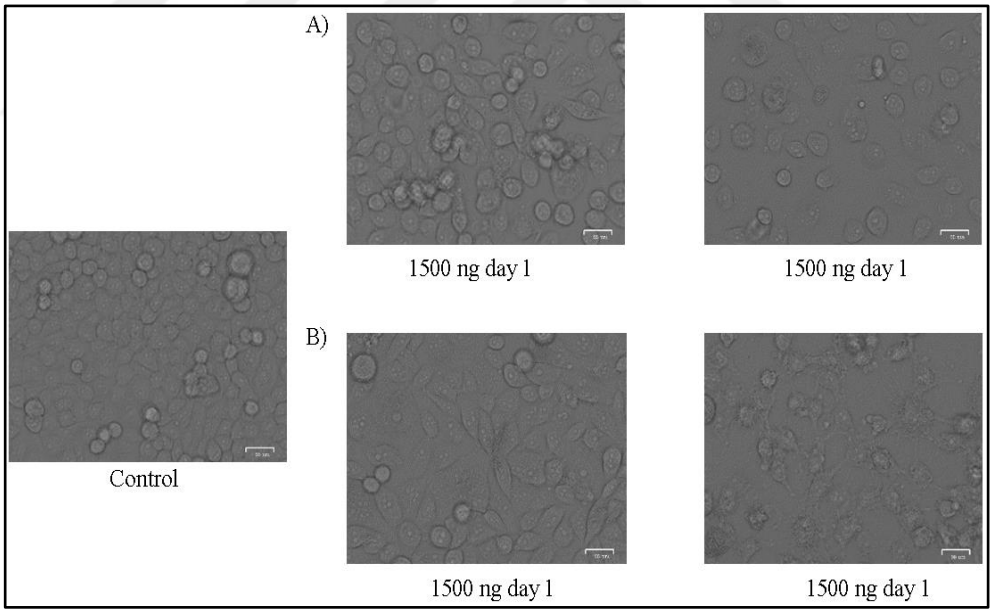

Figure 3. 21: After 48 h of second transfection on PC3 prostate cancer cells, transfected cells were selected with selected doses of Puromycin. Controls were maintained with complete RPMI. a) 1500 ng of puromycin was applied on 2:3 transfected PC3 cells for 48 h. b) 1500 ng of puromycin was applied on 2:3 transfected PC3 cells for 48 h. Cells were observed by brightfield mode of fluorescence cell imager at 25 nm scale.

After that, CRISPR/Cas9 mediated AMPK knock out on PC3 prostate cancer cells was controlled by immunoblotting. When it was knocked out single cell clones were performed on 96 wells plate.

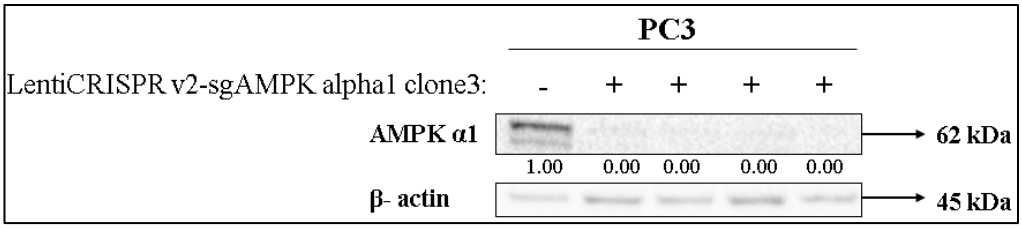

Figure 3. 22: Following the 3 rd day of 1.5µg puromycin treatment the total protein isolation of PC3 cells was performed. AMPK α1 protein expression levels of transfected wells and an untransfected well of PC3 prostate cancer cell was shown. β-actin was used as a loading control.

During single cell process, 4 single clones of PC3 AMPK $^{-/-}$ cells was observed. Their cellular morphologies were determined by brightfield mode of fluorescence cell imager at 25 nm scale.

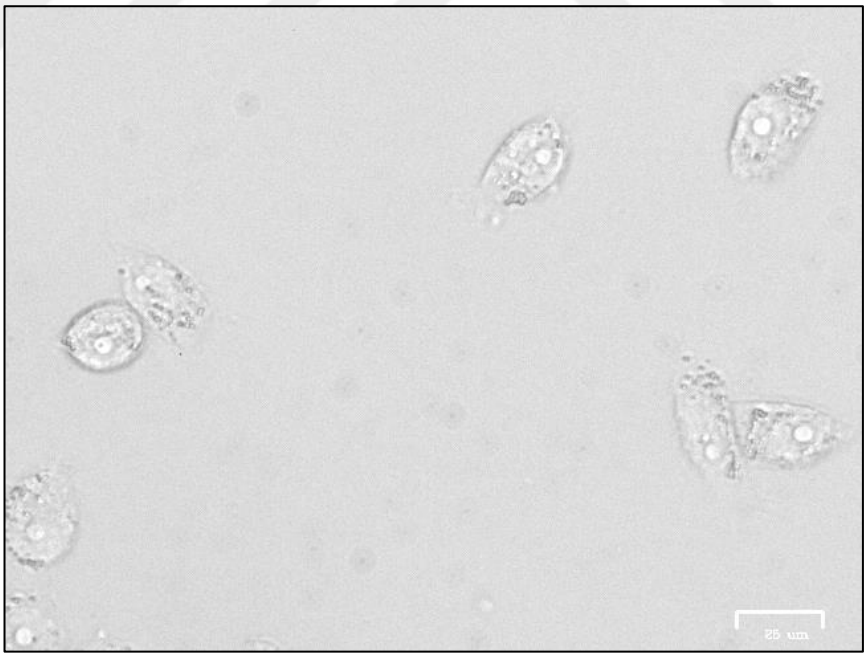

Figure 3. 23: After 15 days from single cell splitting on PC3 AMPK $^{-/-}$ single cell, clone 1 was grown in 24 wells plate. Cells were observed by brightfield mode of fluorescence cell imager at 25 nm scale.

Figure 3. 24: After 15 days from single cell splitting on PC3 AMPK $^{-/-}$ single cell, clone 2 was grown in 24 wells plate. Cells were observed by brightfield mode of fluorescence cell imager at 25 nm scale.

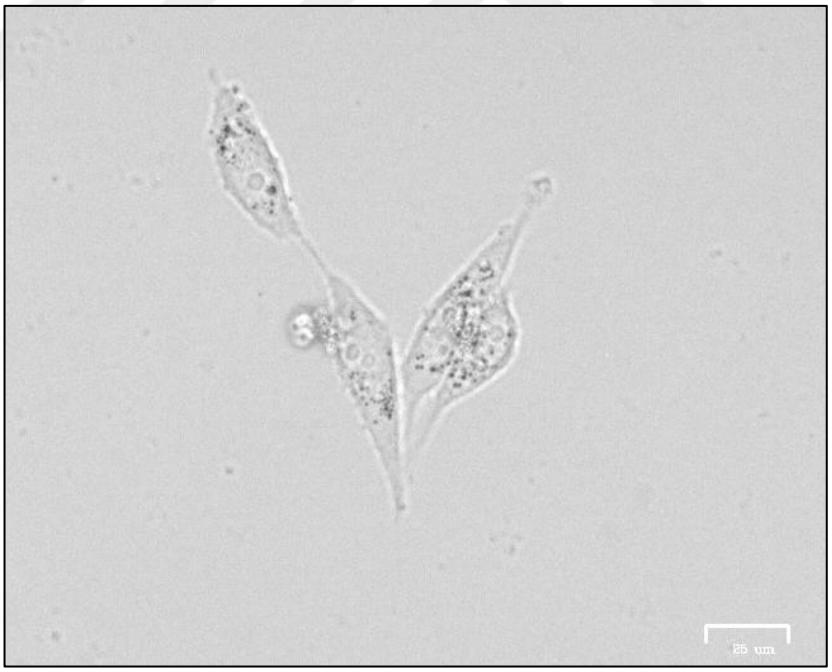

Figure 3. 25: After 15 days from single cell splitting on PC3 AMPK $^{-/-}$ single cell, clone 3 was grown in 24 wells plate. Cells were observed by brightfield mode of fluorescence cell imager at 25 nm scale.

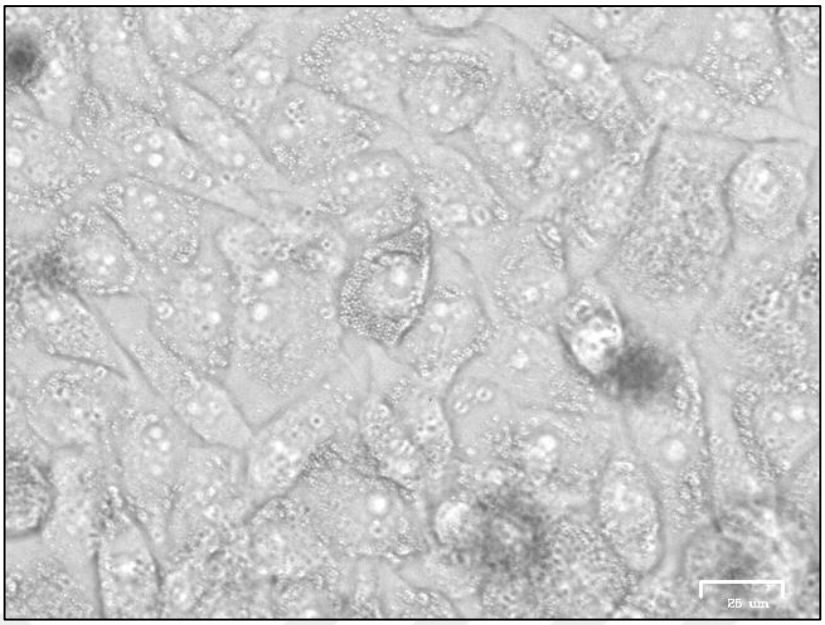

Figure 3. 26: After 15 days from single cell splitting on PC3 AMPK $^{-/-}$ single cell, clone 4 was grown in 24 wells plate. Cells were observed by brightfield mode of fluorescence cell imager at 25 nm scale.

After generation of 4 PC3 AMPK $^{-/-}$ single cell clones, knocking out of AMPK α1 was validated via immunoblotting, which was shown in Figure 3.27. Clone 3 was selected for further experimental procedure.

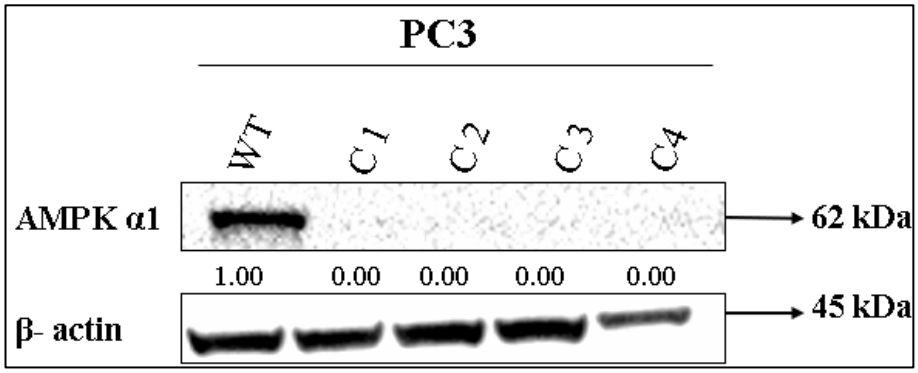

Figure 3. 27: The total protein isolation of PC3 AMPK $^{-/-}$ clones was performed. AMPK α1 protein expression levels of 4 AMPK $^{-/-}$ single cell clones, which were transfected twice with CRISPR/Cas9 mediated lentiviral plasmid, and untransfected cells were compared by immunoblotting. β-actin was used as a loading control.

Then, same protocol was performed on LNCaP cells with 1:6 transfection ratio. After 48h, puromycin selection was applied to select transfected cells over untransfected ones. Figure 3.28 shows the 3rd day of 400 ng puromycin treatment on LNCaP cells. Figure 3.29,3.30 and 3.31 shows the gradual increase of puromycin concentration to select the transfected cells.

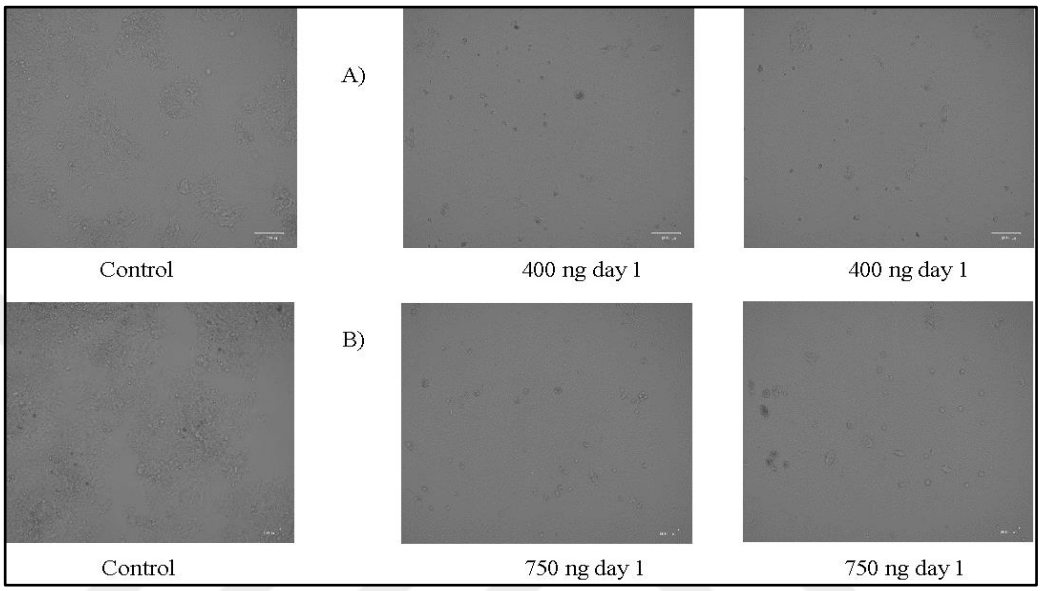

Figure 3. 28: After 48 h of transfection on LNCaP prostate cancer cells, transfected cells were selected with selected doses of Puromycin. Controls were maintained with complete RPMI. a) 400 ng of puromycin was applied on 1:3 transfected PC3 cells for 24 h. b) 750 ng of puromycin was applied on 1:3 transfected LNCaP cells for 24 h. Cells were observed by brightfield mode of fluorescence cell imager at 100 nm scale.

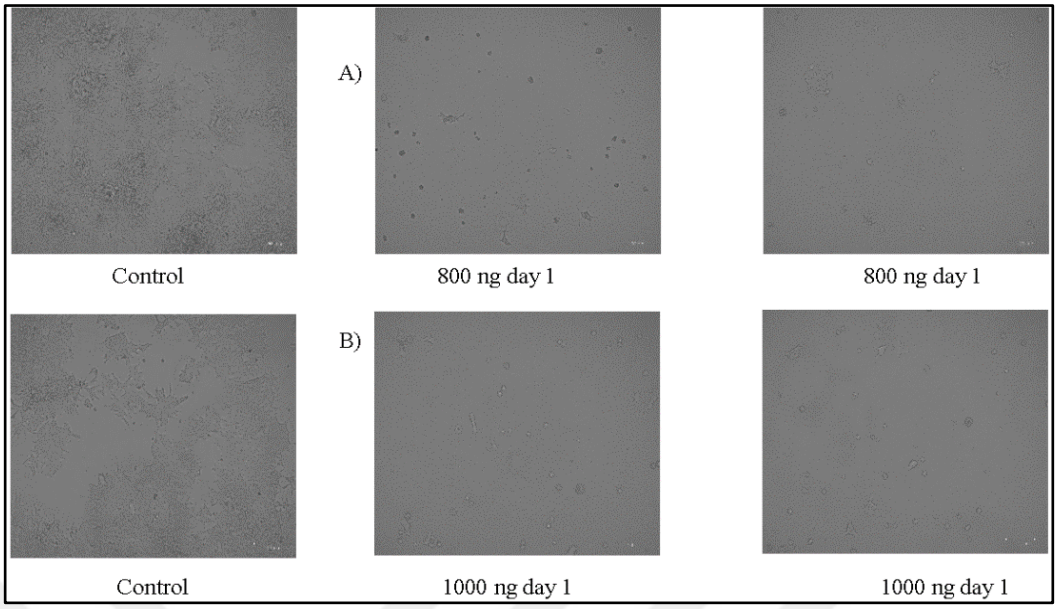

Figure 3. 29: After 48 h of transfection on LNCaP prostate cancer cells, transfected cells were selected with selected doses of Puromycin. Controls were maintained with complete RPMI. a) 400 ng of puromycin was applied on 1:3 transfected LNCaP cells for 24 h. b) 750 ng of puromycin was applied on 1:3 transfected LNCaP cells for 24 h. Cells were observed by brightfield mode of fluorescence cell imager at 100 nm scale.

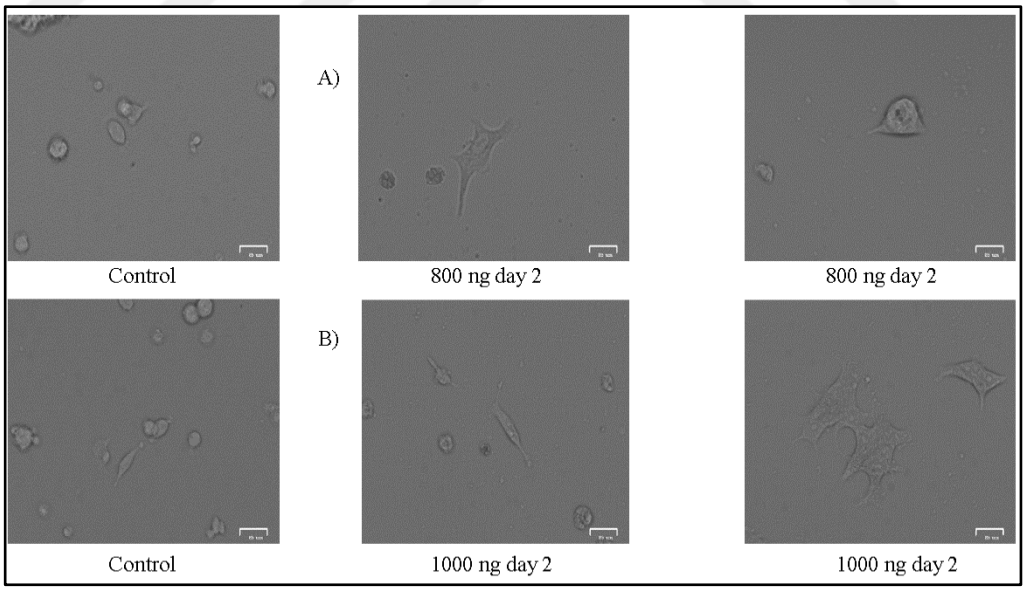

Figure 3. 30: After 48 h of transfection on LNCaP prostate cancer cells, transfected cells were selected with selected doses of Puromycin. Controls were maintained with complete RPMI. a) 800 ng of puromycin was applied on 1:3 transfected LNCaP cells for 48 h. b) 1000 ng of puromycin was applied on 1:3 transfected LNCaP cells for 48 h. Cells were observed by brightfield mode of fluorescence cell imager at 100 nm scale.

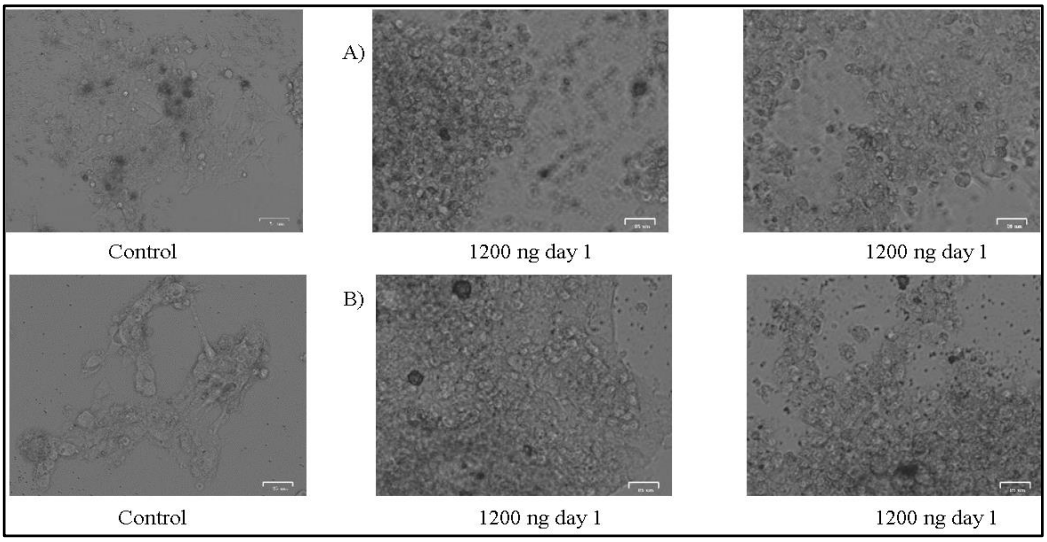

Figure 3. 31: After 48 h of transfection on LNCaP prostate cancer cells, transfected cells were selected with selected doses of Puromycin. Controls were maintained with complete RPMI. a) 1200 ng of puromycin was applied on 1:3 transfected LNCaP cells for 24 h. b) 1200 ng of puromycin was applied on 1:3 transfected LNCaP cells for 24 h. Cells were observed by brightfield mode of fluorescence cell imager at 100 nm scale.

When the puromycin selection reached 1200 ng, AMPK α1 expression levels of LNCaP cells were measured by immunoblotting, which were shown in Figure 3.32.

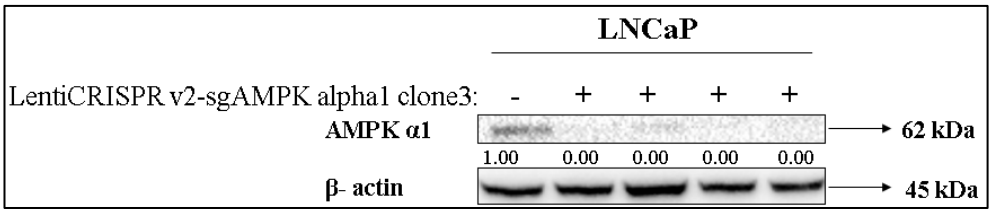

Figure 3. 32: Following the 1 st day of 1.2µg puromycin treatment the total protein isolation of LNCaP cells was performed. AMPK α1 protein expression levels of transfected wells and an untransfected well of PC3 prostate cancer cell was shown. β-actin was used as a loading control.

Then, first well of LNCaP transfected cells was selected and single cell dilution was performed on 96 wells plate to obtain single cell. Unfortunately, single cells couldn't grow and died after 3 weeks. Study was carried out with multiple clones, which was shown in Figure 3.33.

Figure 3. 33: After 15 days from single cell splitting on LNCaP AMPK $^{-/-}$ single cell, clone 1 was grown in 24 wells plate. Cells were observed by brightfield mode of fluorescence cell imager at 27 nm scale.

After ensuring of growth of LNCaP AMPK $^{-/-}$ cells, we validated the silencing process again to make sure the knocking out of AMPK α1 on LNCaP cells. Figure 3.34 shows CRISPR/Cas9 mediated AMPK knock out on LNCaP prostate cancer cells with 1:6 transfection ratio by LentiCRISPR v2-sgAMPK alpha1 clone3. Generated and selected clone was named as Clone 1.

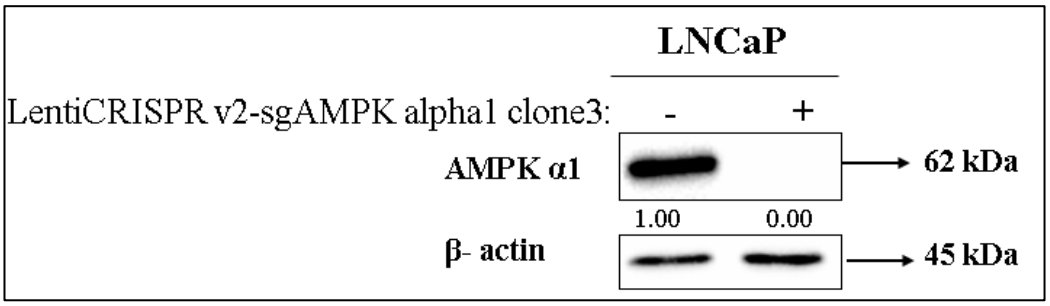

Figure 3. 34: The total protein isolation of LNCaP AMPK $^{-/-}$ clones was performed. AMPK α1 protein expression levels of 4 AMPK $^{-/-}$ single cell clones, which were transfected twice with CRISPR/Cas9 mediated lentiviral plasmid, and untransfected cells were compared by immunoblotting. β-actin was used as a loading control.

3.3. Dose Optimization of Orlistat with MTT Assay on PC3

In order to understand the effect of Orlistat on cell viability, cells were treated with different concentrations of Orlistat (0-100 μM) for 24 h. After generation of PC3 AMPK $^{-/-}$ and LNCaP AMPK $^{-/-}$ cell lines, the dose of orlistat was optimized by considering the cellular toxicity with MTT assay, which was shown as Figure 3.35.

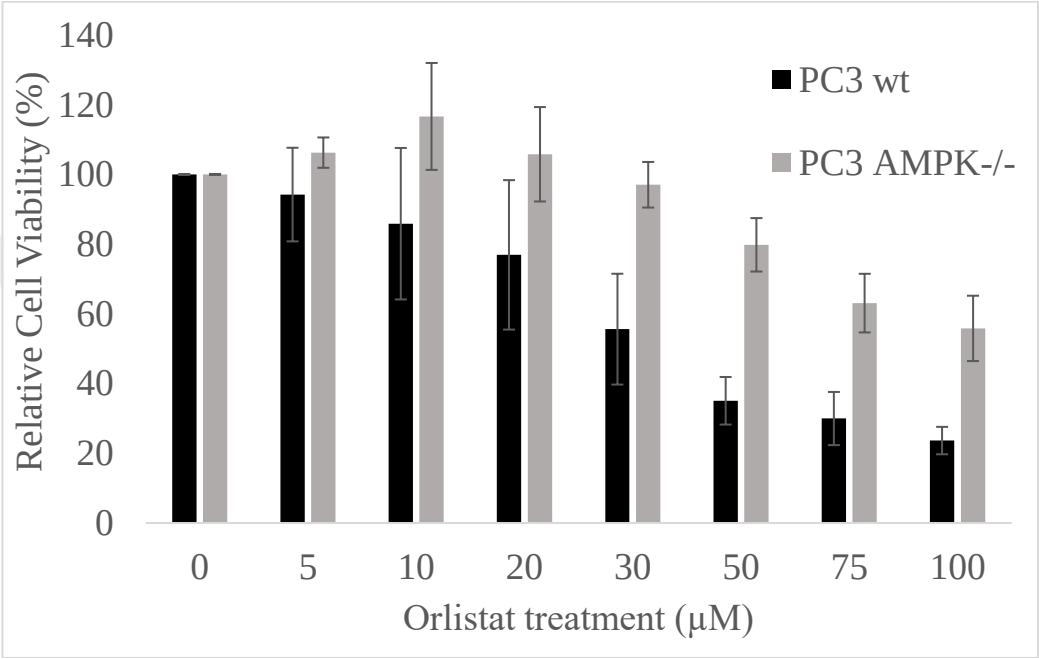

Figure 3. 35: MTT cell viability assay of PC3 wt and AMPK $^{-/-}$ prostate cancer cells was proceeded to evaluate cytotoxic responses against 7 different concentrations (0-100 μM) of Orlistat for 24 h. Columns represent the mean ± standard deviation of three independent experiments with at least four repeats.

At 30 μM concentration, Orlistat decreased cell viability approximately 55% on androgen and PSA independent PC3 (AR-) prostate cancer cells for 24 h of treatment.

3.4. Colony Formation Potential of PC3 and LNCaP Cells Treated with Orlistat

Clonogenic assay was performed on PC3 and LNCaP wt and AMPK $^{-/-}$ cells to see its ability to undergo “unlimited” division and determine the effectiveness of Orlistat.

We observed the reduction of number of colonies for both PC3 and LNCaP wt cells when we applied 0-75 μM range of Orlistat, which were shown in Figure 3.36.

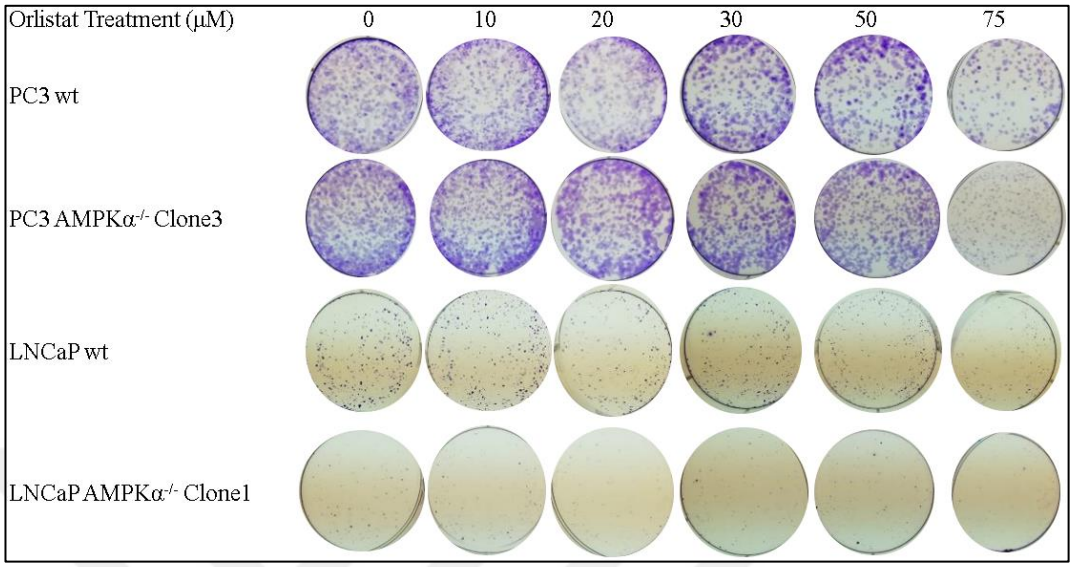

Figure 3. 36: Colony formation assay for PC3 WT, AMPK$^{-/-}$ and LNCaP WT, AMPK$^{-/-}$ top to bottom with different levels of Orlistat. Orlistat suppressed colony formation of PC3 WT, AMPK$^{-/-}$ and LNCaP WT, AMPK$^{-/-}$. After selected concentrations of Orlistat treatment, cells were allowed to form colonies, which were observed with crystal violet staining, in fresh medium for 14 days.

Shrinkage and reduction of colonies on both PC3 and LNCaP AMPK $^{-/-}$ cells were observed when applied 0-75 μM of range of Orlistat for 24 h, which were shown in Figure 3.36. It was found that the colonies got shrink and the number of colonies decreased when the dose increased, for both cell lines. Besides, the results of MTT are consistent with colony formation assay, therefore the optimum 30μM dose of orlistat was validated for both PC3 and LNCaP cells.

3.5. BODIPY Staining for the Observation of Lipid Droplets

PC3 and LNCaP prostate cancer cells were stained with BODIPY stain to observe the amount and the location of lipid droplets before and after the Orlistat treatment, which is shown in Figure 3.37.

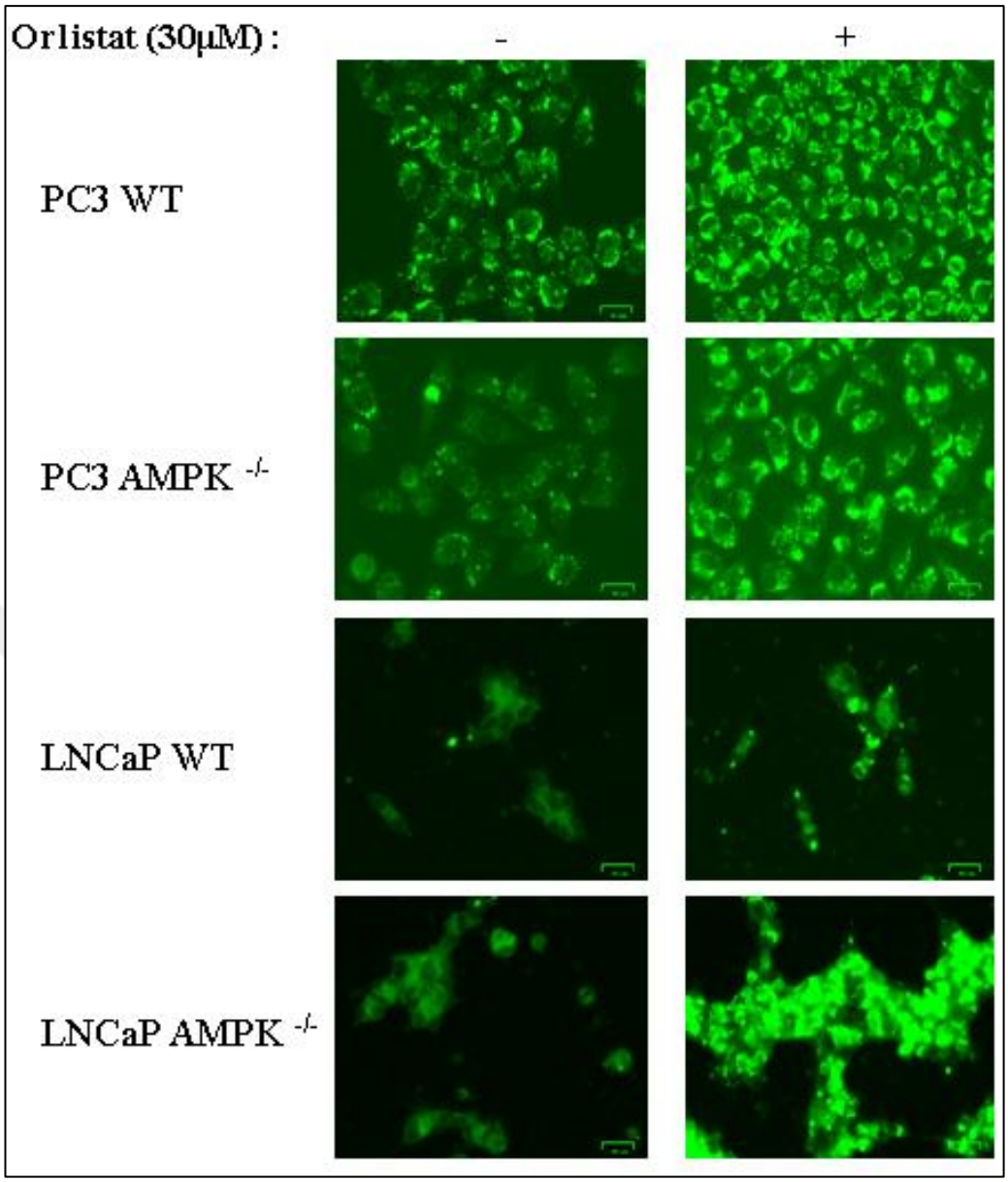

Figure 3. 37: Staining of neutral lipid droplets with BODIPY on PC3 WT, AMPK$^{-/-}$ and LNCaP WT, AMPK$^{-/-}$. 3x10^4 cells were seeded into 24 wells plate and treated with 30 µM Orlistat for 24 h. Neutral lipid droplets were evaluated by BODIPY staining. Cells were observed by fluorescence microscopy at 25 nm.

It was shown that after 24h treatment on PC3 wt and AMPK $^{-/-}$ and LNCaP wt and AMPK $^{-/-}$ cells, the amount of lipid droplets increased relative of untreated ones. Besides, the localization of lipid droplets on LNCaP cells is at the edge of cells.

3.6. DIOC6 and PI Staining for the Observation of Mitochondrial Activity and Dead Cells

Cells were stained with PI and DIOC6 stain to observe the apoptotic cell death in prostate cancer cell population and mitochondrial membrane potential of population.

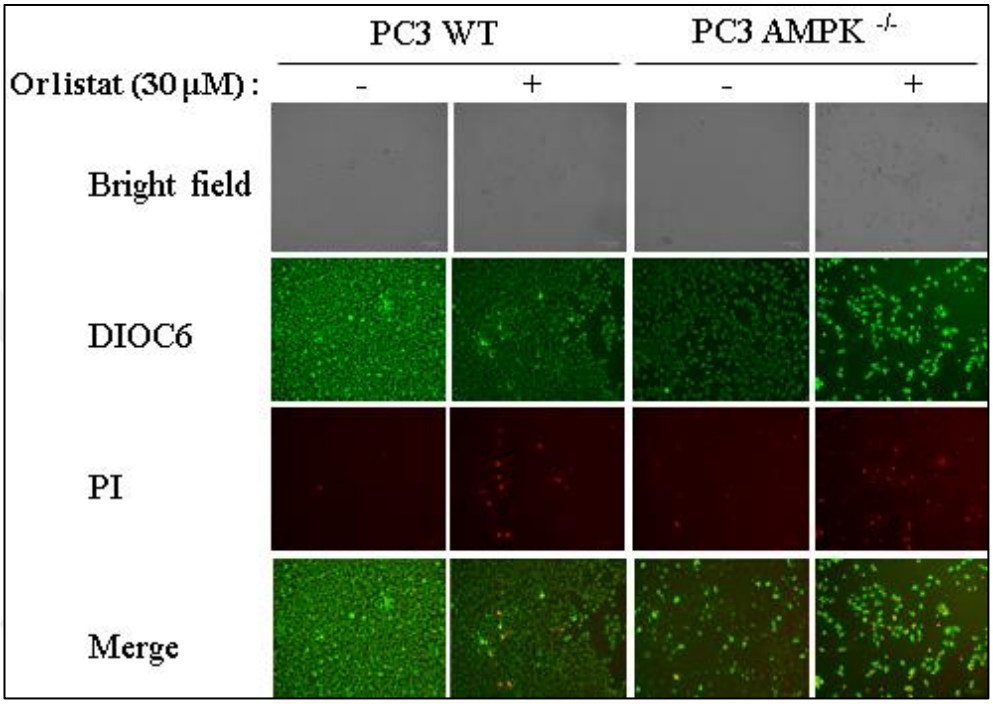

Figure 3. 38: Orlistat induced apoptotic effect through mitochondrial pathway. $3x10^4$ of PC3 WT and $AMPK^{-/-}$ prostate cancer cells were seeded into 24 wells plate ant treated with Orlistat (30 μM) for 24 h. Cytotoxic effect of Orlistat was determined by PI staining. Alteration of mitochondrial membrane potential was evaluated by DIOC6 stain. Scale bars represent 100 nm.

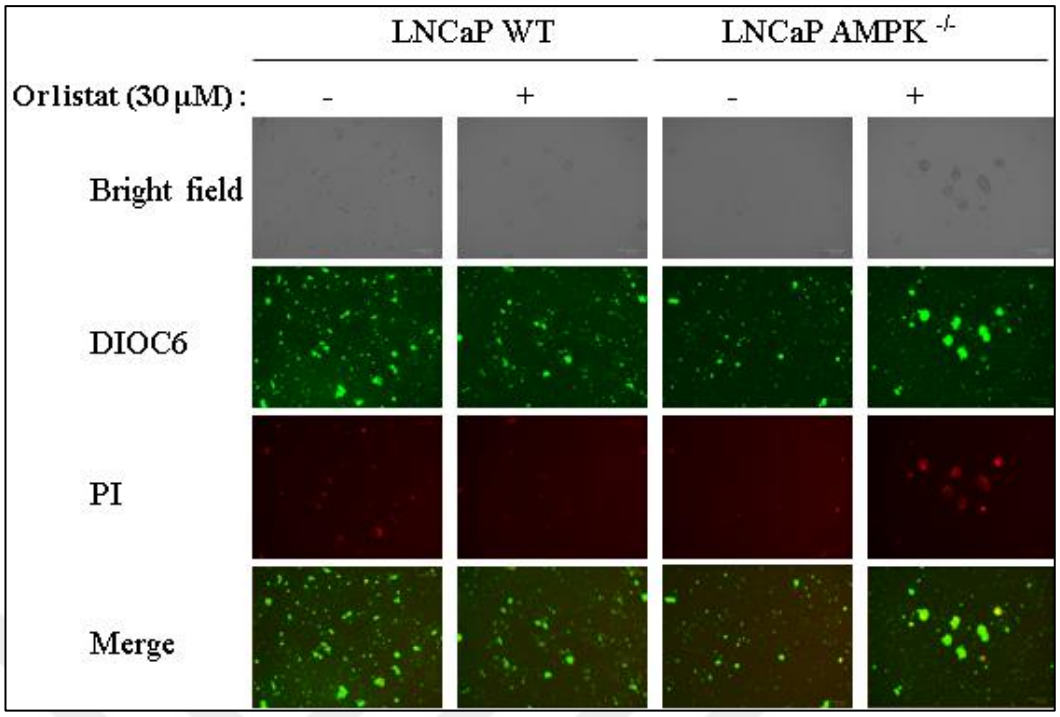

Figure 3. 39: Orlistat induced apoptotic effect through mitochondrial pathway. $3x10^4$ of LNCaP WT and $AMPK^{-/-}$ prostate cancer cells were seeded into 24 wells plate ant treated with Orlistat (30 µM) for 24 h. Cytotoxic effect of Orlistat was determined by PI staining. Alteration of mitochondrial membrane potential was evaluated by DIOC6 stain. They were observed by fluorescence microscopy at 100 nm.

It was shown that for both PC3 and LNCaP cells, orlistat increases the death rate. It was observed that AMPK $^{-/-}$ PC3 and LNCaP cells are more vulnerable to orlistat because their death rate is increased relative of wt cells.

3.7. Protein Expression Profiles of PC3 and LNCaP cells with Orlistat Treatment

In order to understand the potential role of Orlistat on cell survival, proliferation and cell death, 30μM of Orlistat treatment was performed on both LNCaP and PC3 cells for 24 h to identify potential targets of orlistat dependent on AMPK deprivation, which was shown in Figure 3.41 and Figure 3.42.

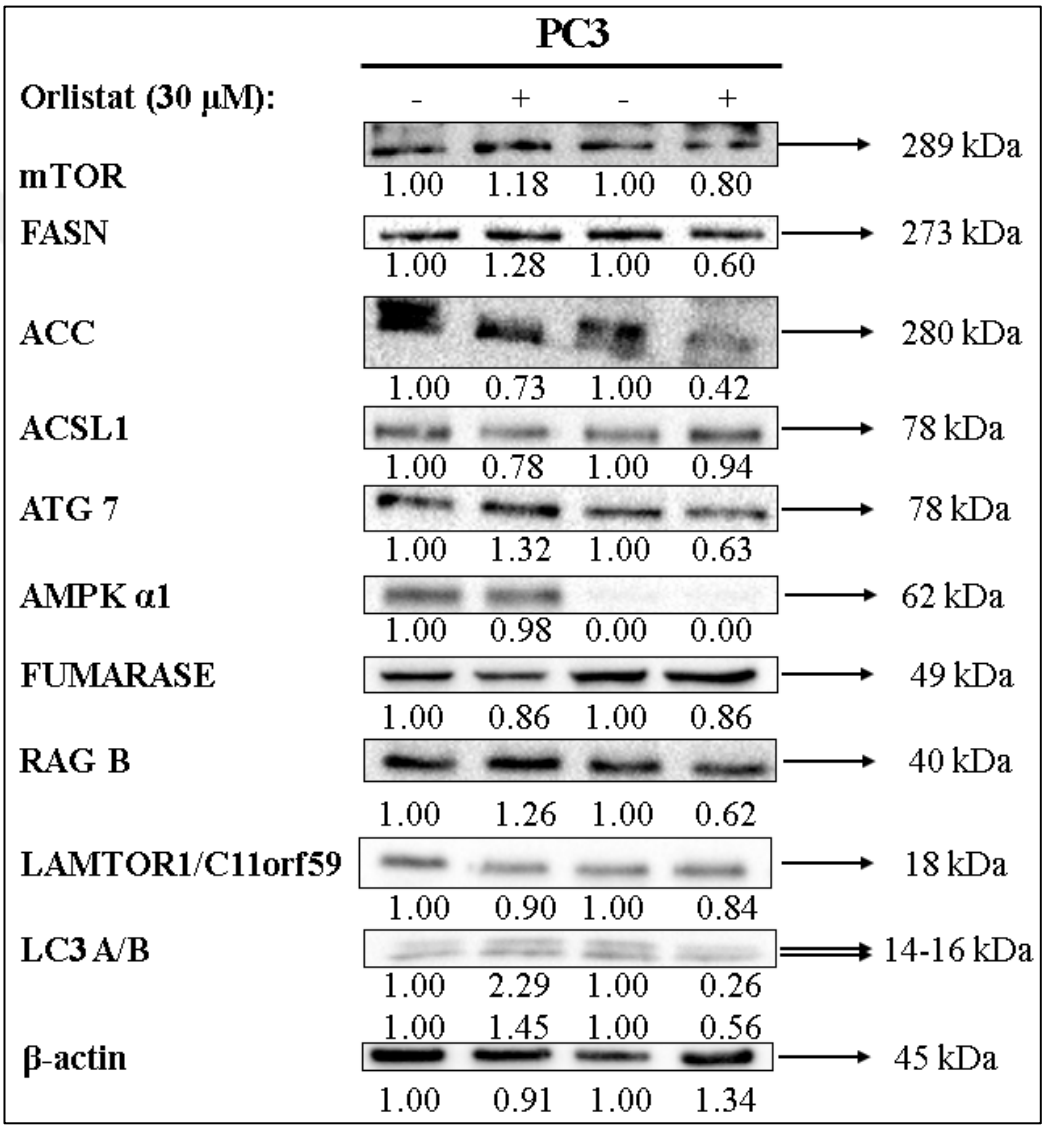

Figure 3. 40: Modulation of the molecular targets of fatty acid synthesis, cell survival and autophagy pathways, which are the molecular targets that are altered by Orlistat treatment on PC3 and AMPK $^{-/-}$ were shown by immunoblotting. Following 24 h of total proteins were isolated and separated in 10% SDS-PAGE, blotted in PVDF membrane. β-actin was used as a loading control.

Firstly, the knocking out of AMPK via CRISPR/Cas9 gene editing, on PC3 prostate cancer cell was determined to check the AMPK levels of PC3 prostate cancer cells. Orlistat is a lipase inhibitor that blocks lipid biogenesis by inhibiting FASN. Therefore, expression of FASN was observed to test the activity of orlistat. In the study, FASN is upregulated on PC3 wt for 24 h Orlistat treatment. In the case of AMPK deficiency, FASN is downregulated when cells treated with orlistat for 24 h. Orlistat promotes and maintains weight loss by changing lipid metabolism. After orlistat treatment, ACC and ACSL1 are both downregulated on both wt and AMPK $^{-/-}$. When autophagy perspective was considered, one of the most important autophagy markers, which are ATG7 and LC3 levels were determined. Although, ATG7 is upregulated on PC3 wt cells for 24 h orlistat treatment, it was downregulated in the case of AMPK deficiency. Although, A fragment of LC3 was upregulated on PC3 wt for 24 h orlistat treatment, in the case of AMPK deficiency, it was downregulated. As for B fragment of LC3, it was downregulated on PC3 wt and upregulated for AMPK deficiency. Orlistat is known for its anti-proliferative activity, therefore, mTOR, RAG B and LAMTOR1/C11orf59 was investigated. mTOR is upregulated on PC3 wt cells. In the case of AMPK deficiency, it is downregulated. RAGB, which is an important molecule for the activity of mTOR, is upregulated on PC3 wt and downregulated on the AMPK $^{-/-}$ PC3 prostate cancer cell. As for LAMTOR1/C11orf59, which is another important molecule for the activity of mTOR, is downregulated on both PC3 wt cells and AMPK deficiency after 24 h of Orlistat treatment.

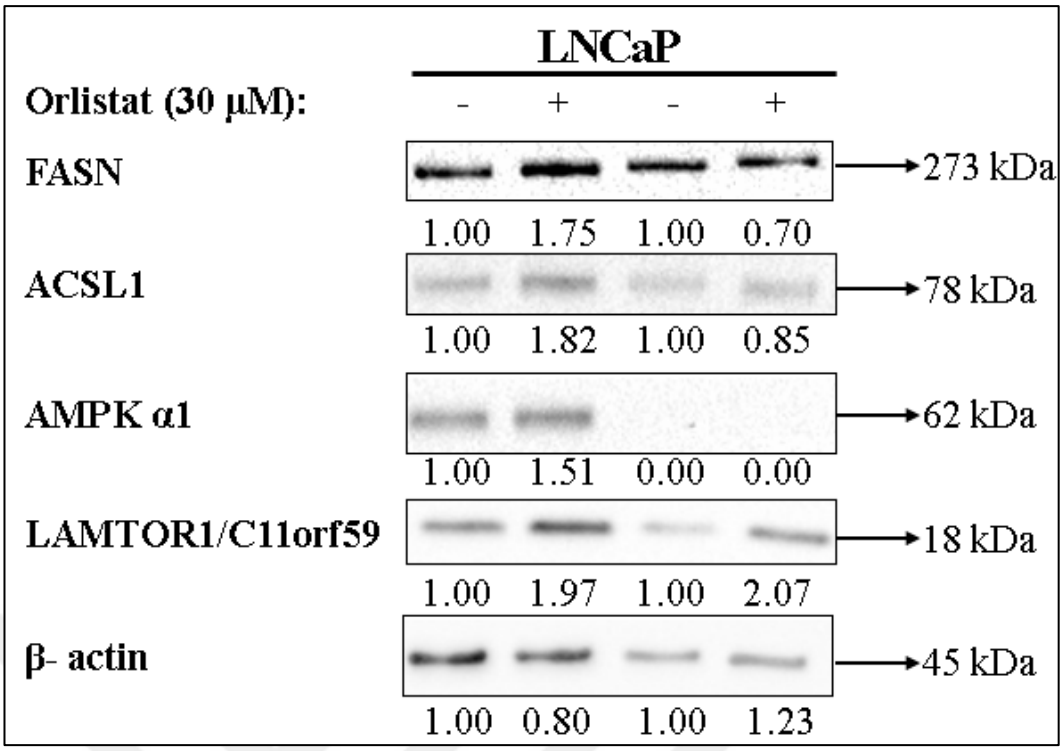

Figure 3. 41: Modulation of the molecular targets of fatty acid synthesis, cell survival and autophagy pathways, which are the molecular targets that are altered by Orlistat treatment on LNCaP and AMPK $^{-/-}$ were shown by immunoblotting. Following 24 h of total proteins were isolated and separated in 10% SDS-PAGE, blotted in PVDF membrane. β-actin was used as a loading control.

Firstly, the knocking out of AMPK via CRISPR/Cas9 gene editing, on LNCaP prostate cancer cell was determined to check the AMPK levels of PC3 prostate cancer cells. FASN is upregulated on LNCaP wt for 24 h of Orlistat treatment. In the case of AMPK deficiency, it was downregulated. Although, ACSL1 is upregulated on LNCaP wt for 24 h of Orlistat treatment, it was downregulated on the case of AMPK deficiency. LAMTOR1/C11orf59 is upregulated on both LNCaP WT and AMPK $^{-/-}$ after 24 h of Orlistat treatment.

4. DISCUSSION and CONCLUSION

Prostate cancer is the most common cancer in the world and one of the leading causes of cancer related- deaths [1], [3]. There are several risk factors that triggers the development of prostate cancer, such as genetic susceptibility, age, nutrition. According to Otto Warburg, cancer cells exert not only increased glycolysis and glutaminolysis but also *de novo* lipogenesis. Most cancers, fatty acid synthesis enzymes are upregulated and their downregulation cause anti-tumor effects [4]. Therefore, metabolic changes of prostate cancer are one of the most intriguing research subjects. The progression of cancer cell is dependent on the metabolic changes; therefore, it is stated that metabolic changes can be a promising target for cancer therapies [27], [29]. In this study, we targeted lipogenesis especially fatty acid synthase enzyme to understand the effect of such metabolic changes on prostate cancer.

In this thesis, we generated AMPK $^{-/-}$ PC3 and LNCaP cell lines, which provide a cell line model with energy sensor deficiency. AMPK is not only an energy sensor but also it has dual role which is both tumor suppressor and an oncogene.

During knocking out, puromycin was used as selectable marker to select transfected cells over untransfected ones. It is important to check the transfection state of cells during puromycin selection. Sometimes, the concentration of DNA may not be sufficient, and it may be required to increase the concentration of lentiviral vector to cut the specific site of genome. We applied 200 - 2000 ng range of puromycin concentration by changing the media of cells and monitored cells and observed the death of untransfected cells. There was no significant change in morphology of PC3 after transfection. The ability of adherence of LNCaP decreased significantly after being stable AMPK $^{-/-}$. We saw that they gain more and more tendency to become cluster after being stable and nearly lost the ability of being adherent. Besides, their rate of growth decreased after being AMPK deficit.

In the study, Orlistat was used, which is quite common drug, which acts on FASN as a molecular target, that is used especially as an anti-obesity agent. It has a blockade role on cell cycle progression, and it promotes apoptotic cell death on various cancers [29]. There are other alternatives of Orlistat, such as C75 and Tofa but their bioavailability and toxicity on cells, limits their clinical usage [31].

After generation of AMPK $^{-/-}$ stable cell line, the dose of orlistat was optimized by MTT assay. Although, we saw 30 μM of orlistat is the most optimum dose for PC3 and LNCaP wt cells, we require 50 μM of orlistat to efficient death of AMPK $^{-/-}$. We observed 70% cell viability when cells treated with 30 μM of orlistat. According to the similar study that was performed on pancreatic cancer cells, especially on PANC-1, 30 μM of orlistat treatment for 72 h was optimal dose therefore the dose optimization could be considered as consistent in both studies. We could not achieve 72 h of Orlistat treatment because of the massive cell death even on 48 h. Similarly, they observed the downregulation of FASN on mRNA level after 72 h treatment. We could not observe the downregulation of FASN on wt of LNCaP and PC3 on protein expression levels after 24 h treatment on protein expression level. It may be because of the action and metabolization time of Orlistat [32], [33].

Additionally, Orlistat was shown to inhibit lung cancer cell proliferation. They also proved the downregulation of FASN activity on mRNA level. They showed the antiproliferative activity is performed with dose dependent manner by performing colony formation assay therefore it is clear that Orlistat is not only effective on pancreatic and breast cancer but also on lung cancer and has therapeutic potential for treatment of at least 3 different cancer types [31]. They also stated 30 μM of orlistat suppressed cell growth. It means that, selected dose of orlistat is the optimal dose for at least 3 different cancer cell lines [30] [31], [32]. Additionally, in this study, it was shown the reduced number and shrinkage of colonies on both PC3 (AR-) and LNCaP (AR+) prostate cancer cells.

Then, BODIPY staining was performed to obtain the amount and location of lipid droplets after 24 h treatment. 24 h of Orlistat treatment increased lipid droplets after treatment although we applied one of the most common lipase inhibitors. In cancer cells, *de novo* FA synthesis appear to be increased [29], [31]. It can be stated that, 24 h treatment may not be enough to the cellular stress that decrease the amount of lipid droplets. Recent studies showed that 72 h of Orlistat treatment shows inhibitory activity on fatty acid synthesis pathways. During the BODIPY staining, when we compare wt and AMPK $^{-/-}$ PC3 cell lines, we observed the decrease of lipid droplets independent of the orlistat treatment. It proves the regulatory role of AMPK in lipid biosynthesis. Lipid metabolism is downregulated without AMPK, independent of orlistat treatment.

When the neutral lipid droplets in the study was considered as dynamic organelles, which are intracellular structure whose formation and regulation is tightly controlled and affects various types of pathological issues, the increase of them is stated to be toxic for cells and promotes apoptosis dependent on the Orlistat treatment [33]. Recent studies showed that 72 h of Orlistat treatment promotes apoptosis on pancreatic and breast cancer cells [30], [31], [32].

After that, cells were stained with DIOC4 and PI in order to see the mitochondrial activity and rate of death. We observed that, after 24 h of Orlistat treatment, the rate of death significantly increased and mitochondrial activity is decreased. Although, mitochondrial membrane potential is decreased on PC3 wt cells after 24 h of Orlistat treatment, in the case of AMPK deficiency it is increased. It was observed that mitochondrial membrane potential is decreased on LNCaP cells independent on AMPK deficiency. It is consistent with the neutral lipid droplet staining that shows the induction of apoptosis.

After total protein isolation following 30 μM concentration of orlistat treatment for 24 h, molecular targets of orlistat were identified dependent on AMPK silencing by investigating protein expression profiles. When we search for the protein expression levels of PC3 and LNCaP, we validated the stability of the knocking out of AMPK urgently. Orlistat is an irreversible inhibitor of pancreatic and gastric lipases, used as an anti- obesity agent by inhibiting FASN activity that's why it directly acts on lipid metabolism. In the study, FASN is upregulated on PC3 and LNCaP wt cells after 24 h of Orlistat treatment. It may have happened because of the time of treatment. In recent studies, researchers, treated the cells for 72 h to generate significant amount of stress that induce inhibition of fatty acid biosynthesis [27], [29]. In the study, sufficient amount of stress that induce the inhibition of FASN may not have been generated with 24 h of Orlistat treatment [27], [29], [32], [33]. It is consistent with the neutral lipid staining experiment on wt of PC3 and LNCaP, which shows the increase of neutral lipid droplets. 24 h of Orlistat treatment on wt of PC3 and LNCaP prostate cancer cells, did not downregulate FASN protein, which appears as an augmentation of neutral lipid droplets. The neutral lipid augmentation can be suggested as promotion of apoptosis, whose induction is managed by toxic effects of neutral lipid droplets. In the case of AMPK deficiency, 30 μM concentration of orlistat treatment for 24 h downregulates FASN, which is the central molecule of lipid biosynthesis, that is inhibited by AMPK.

ACSL1 is known for the promoter of uncontrolled cell growth and facilitator of tumor invasion and escaper from apoptosis [34]. ACSL1 for being long fatty acid chain activator, is downregulated on both wt of PC3 and AMPK $^{-/-}$ after 30μM concentration of orlistat treatment for 24 h. Although ACSL1 is upregulated on wt of LNCaP, it is downregulated in AMPK deficiency. It means AMPK deficiency has a role for the activity of Orlistat on the alteration of lipid metabolism.

Orlistat has anti-proliferative activity on cancer cells therefore protein synthesis and cell survival markers were evaluated after 30μM concentration of orlistat treatment for 24 h. LAMTOR1/C11orf59, is one of the components of Ragulator complex, that tethers mTORC1, with LAMTOR 2, 3,4 and 5. LAMTOR 1-5, indirectly regulates protein synthesis and cell survival. Although, Lamtor1/C11orf59 was found downregulated on both PC3 wt and AMPK $^{-/-}$, it was found upregulated on both LNCaP wt and AMPK $^{-/-}$ prostate cancer cells after 30μM concentration of orlistat treatment for 24 h. It can be suggested that LNCaP compensates the negative regulative role of Orlistat on cell survival and proliferation via protein synthesis pathways, specifically LAMTOR1/C11orf59 [27], [31], [32]. mTOR is one of the most important cell survival and proliferation marker with RAGB, which is an important component of Ragulator complex for the activity of mTOR, they were found as upregulated on wt of PC3 cells and downregulated on AMPK deficient PC3 prostate cancer cells. It can be said that AMPK deficiency might increase the effect of Orlistat for 24 h interval via protein synthesis pathways.

Autophagy markers were investigated to understand the effect of Orlistat, we saw an upregulation in the levels of ATG7, which is one of the components of phagophore, on PC3 wt cells after 24 h of Orlistat treatment. In the case of AMPK deficiency, ATG7 is downregulated. A fragment of LC3 is upregulated on PC3 wt after 24 h of treatment and downregulated in the case of AMPK deficiency. As for B fragment, it was upregulated on wt and downregulated on AMPK deficiency. It can be suggested that AMPK has a role on drug resistance for Orlistat [27]. FUMARASE is known as the mitochondrial enzyme that catalyzes fumarate to malate and its deficiency is associated with renal cancer [36]. It can be considered as a tumor suppressor and after orlistat treatment it was downregulated on AMPK $^{-/-}$ PC3 prostate cancer cells. Lipid oxidation markers need further investigation for being tumor suppressor proteins.

For further experiments, we may end the treatment 72 h to observe the relatively long-term effect of Orlistat on lipid biogenesis and metastatic profile of cancer. Besides, we can perform the experiments not only see the apoptosis but also for ferroptosis, which is a type of programmed cell death characterized by the accumulation of lipid peroxides especially by observing ferroptosis markers [31], [37]. Lipid metabolism was the main target for the study for monitoring the alteration of prostate cancer metabolism, that's why lipid peroxidation and formation of reactive oxygen species should be promising targets for the treatment of prostate cancer.

AMPK could be a useful target for PCa. Decreased cell viability and colony formation potential because of orlistat treatment shows that orlistat treatment can be a useful therapeutic approach to treat prostate cancer in a dose dependent manner. Although we highlighted the therapeutic potential of orlistat on prostate cancer cells, molecular targets, mechanisms, and novel genes that were affected by the treatment need further investigation.

REFERENCES

[1] Pernar, C., Ebot, E., Wilson, K., & Mucci, L., (2018), "The Epidemiology of Prostate Cancer", Cold Spring Harbor Perspectives In Medicine, 8(12), a030361. doi: 10.1101/cshperspect.a030361.

[2] Sandhu, S., Moore, C., Chiong, E., Beltran, H., Bristow, R., Williams, S., (2021), "Prostate cancer", The Lancet, 398(10305), 1075-1090.

[3] Schatten, H., (2018), "Brief Overview of Prostate Cancer Statistics, Grading, Diagnosis and Treatment Strategies", Advances In Experimental Medicine And Biology, 1095(1), 1-14.

[4] Grozescu, T., & Popa, F., (2017), "Prostate cancer between prognosis and adequate/proper therapy", Journal of medicine and life, 10(1), 5–12.

[5] Chang, A., Autio, K., Roach, M., & Scher, H., (2014), "High-risk prostate cancer—classification and therapy", Nature Reviews Clinical Oncology, 11(6), 308-323.

[6] Davies, N., Gaunt, T., Lewis, S., Holly, J., Donovan, J., & Hamdy, F. et al., (2015), "The effects of height and BMI on prostate cancer incidence and mortality: a Mendelian randomization study in 20,848 cases and 20,214 controls from the PRACTICAL consortium", Cancer Causes &Amp; Control, 26(11), 1603-1616.

[7] Haberkorn, U., Eder, M., Kopka, K., Babich, J., & Eisenhut, M., (2016), "New Strategies in Prostate Cancer: Prostate-Specific Membrane Antigen (PSMA) Ligands for Diagnosis and Therapy", Clinical Cancer Research, 22(1), 9-15.

[8] D. P. Mikhailidis, (2010), "Expert Opinion on Pharmacotherapy: Foreword," Expert Opinion on Pharmacotherapy, 11(16), 2573,

[9] Nevedomskaya, E., Baumgart, S., & Haendler, B., (2018), "Recent Advances in Prostate Cancer Treatment and Drug Discovery", International Journal of Molecular Sciences, 19(5), 1359.

[10] Komura, K., Sweeney, C., Inamoto, T., Ibuki, N., Azuma, H., & Kantoff, P., (2017), "Current treatment strategies for advanced prostate cancer", International Journal Of Urology, 25(3), 220-231.

[11] Shorning, B., Dass, M., Smalley, M., & Pearson, H., (2020), "The PI3K-AKT-mTOR Pathway and Prostate Cancer: At the Crossroads of AR, MAPK, and WNT Signaling", International Journal Of Molecular Sciences, 21(12), 4507.

[12] M. Palmieri et al., (2017), “mTORC1-independent TFEB activation via Akt inhibition promotes cellular clearance in neurodegenerative storage diseases,” Nature Communications, 8(3), 567.

[13] Goldar, S., Khaniani, M., Derakhshan, S., & Baradaran, B., (2015), “Molecular Mechanisms of Apoptosis and Roles in Cancer Development and Treatment”, Asian Pacific Journal of Cancer Prevention, 16(6), 2129-2144.

[14] Herzig, S., & Shaw, R., (2017), “AMPK: guardian of metabolism and mitochondrial homeostasis”, Nature Reviews Molecular Cell Biology, 19(2), 121-135.

[15] Russell, F., & Hardie, D., (2020), “AMP-Activated Protein Kinase: Do We Need Activators or Inhibitors to Treat or Prevent Cancer?”, International Journal of Molecular Sciences, 22(1), 186.

[16] D. Vara-Ciruelos, F. M. Russell, and D. Grahame Hardie, (2019) “The strange case of AMPK and cancer: Dr Jekyll or Mr Hyde?,” Open Biology, 9(7), 258-265.

[17] Russell, F., & Hardie, D., (2020), “AMP-Activated Protein Kinase: Do We Need Activators or Inhibitors to Treat or Prevent Cancer?”, International Journal Of Molecular Sciences, 22(1), 186.

[18] D. Vara-Ciruelos, F. M. Russell, and D. Grahame Hardie, (2019),“The strange case of AMPK and cancer: Dr Jekyll or Mr Hyde?”, Open Biology, 9(7), Royal Society Publishing, 9(7), 258-265.

[19] Wang, Z., Wang, N., Liu, P., & Xie, X., (2016), “AMPK and Cancer”, Experientia Supplementum, 25(1), 203-226.

[20] Kim, J., Yang, G., Kim, Y., Kim, J., & Ha, J.,(2016), “AMPK activators: mechanisms of action and physiological activities”, Experimental &Amp; Molecular Medicine, 48(4), e224-e224.

[21] Kinaan, M., Ding, H., & Triggle, C., (2015), “Metformin: An Old Drug for the Treatment of Diabetes but a New Drug for the Protection of the Endothelium”, Medical Principles And Practice, 24(5), 401-415.

[22] Gong, L., Goswami, S., Giacomini, K., Altman, R., & Klein, T., (2012), “Metformin pathways”, Pharmacogenetics and Genomics, 22(11), 820-827.

[23] Heck, A., Yanovski, J., & Calis, K., (2000), “Orlistat, a New Lipase Inhibitor for the Management of Obesity”, Pharmacotherapy, 20(3), 270-279.
[24] W. McNeely, P. Benfield, L. Drent, and F. X. Pi-Sunyer, “Orlistat,” *Drugs*, vol. 56, no. 2, pp. 241–249, 1998, doi: 10.2165/00003495-199856020-00007.

[25] Borgström, B., (1988), “Mode of action of tetrahydrolipstatin: a derivative of the naturally occurring lipase inhibitor lipstatin”, Biochimica Et Biophysica Acta (BBA) - Lipids And Lipid Metabolism, 962(3), 308-316.

[26] Schcolnik-Cabrera, A., Chávez-Blanco, A., Domínguez-Gómez, G., Taja-Chayeb, L., Morales-Barcenas, R., & Trejo-Becerril, C. et al., (2018), “Orlistat as a FASN inhibitor and multitargeted agent for cancer therapy”, Expert Opinion On Investigational Drugs, 27(5), 475-489.

[27] A. Schcolnik-Cabrera *et al.*, “Orlistat as a FASN inhibitor and multitargeted agent for cancer therapy,” *Expert Opin Investig Drugs*, vol. 27, no. 5, pp. 475–489, May 2018, doi: 10.1080/13543784.2018.1471132.

[28] Rasband, W.S., ImageJ, U. S. National Institutes of Health, Bethesda, Maryland, USA, https://imagej.nih.gov/ij/, 1997-2018.

[29] Schcolnik-Cabrera, A., Chávez-Blanco, A., Domínguez-Gómez, G., Taja-Chayeb, L., Morales-Barcenas, R., & Trejo-Becerril, C. et al., (2018), “Orlistat as a FASN inhibitor and multitargeted agent for cancer therapy”. Expert Opinion On Investigational Drugs, 27(5), 475-489.

[30] Zhou, W., Zhang, J., Yan, M., Wu, J., Lian, S., & Sun, K. et al., (2021), “Orlistat induces ferroptosis-like cell death of lung cancer cells”, Frontiers Of Medicine, 15(6), 922-932.

[31] W. Zhou *et al.*, “Orlistat induces ferroptosis-like cell death of lung cancer cells,” *Front Med*, vol. 15, no. 6, pp. 922–932, Dec. 2021, doi: 10.1007/S11684-020-0804-7.

[32] E. Sokolowska, M. Presler, E. Goyke, R. Milczarek, J. Swierczynski, and T. Sledzinski, “Orlistat Reduces Proliferation and Enhances Apoptosis in Human Pancreatic Cancer Cells (PANC-1),” Anticancer Res, 37(11) 6321–6327.

[33] Menendez J. A., Vellon, L., & Lupu, R., (2005), “Antitumoral actions of the anti-obesity drug orlistat (XenicalTM) in breast cancer cells: blockade of cell cycle progression, promotion of apoptotic cell death and PEA3-mediated transcriptional repression of Her2/neu (erbB-2) oncogene,” Ann Oncol, 16(8) 1253–1267.

[34] Tang, Y., Zhou, J., Hooi, S., Jiang, Y., & Lu, G., (2018), “Fatty acid activation in carcinogenesis and cancer development: Essential roles of long-chain acyl-CoA synthetases” Oncology Letters, 45(11) 631-650 doi: 10.3892/ol.2018.8843

[35] Koukourakis, M., Kalamida, D., Giatromanolaki, A., Zois, C., Sivridis, E., & Pouliliou, S., (2015), “Autophagosome Proteins LC3A, LC3B and LC3C Have Distinct Subcellular Distribution Kinetics and Expression in Cancer Cell Lines”, PLOS ONE, 10(9), e0137675. doi: 10.1371/journal.pone.0137675

[36] Leshets, M., Silas, Y., Lehming, N., & Pines, O., (2018), “Fumarase: From the TCA Cycle to DNA Damage Response and Tumor Suppression”, Frontiers In Molecular Biosciences, 5(11). doi: 10.3389/fmolb.2018.00068

[37] Lee, H., Zhuang, L., & Gan, B., (2020), “Energy stress inhibits ferroptosis via AMPK”, Molecular &Amp; Cellular Oncology, 7(4), 1761242. doi: 10.1080/23723556.2020.1761242

BIOGRAPHY

Ayyüce Sever was completed her bachelor's degree from the Molecular Biology and Genetics program at Gebze Technical University. She performed her internships at Chemistry Department in Gebze Technical University, Pharmacology Department in Marmara University, Molecular Biology and Genetics department in Acıbadem University. Currently, she is working as research assistant in Gebze Technical University. She is also continuing her master's degree program at Biotechnology Institute within Gebze Technical University.